Water Resources Research

RESEARCH ARTICLE

10.1029/2018WR023054

Bayesian Analyses of 17 Winters of Water Vapor Fluxes Show Bark Beetles Reduce Sublimation

John M. Frank[1,2], William J. Massman[1], Brent E. Ewers[2], and David G. Williams[2]

[1]Rocky Mountain Research Station, U.S. Forest Service, Fort Collins, CO, USA, [2]Department of Botany and Program in Ecology, University of Wyoming, Laramie, WY, USA

Key Points:

- Ecosystem sublimation decreased 24% following a spruce beetle outbreak in a subalpine forest in Wyoming, USA
- A Bayesian analysis identified the loss of canopy causing less snow interception as the driver of this change
- This allows the snowpack to retain 6% more mass, an increase that is hydrologically, ecologically, and socially meaningful in this region

Supporting Information:

- Supporting Information S1

Correspondence to:
J. M. Frank,
jfrank@fs.fed.us

Citation:
Frank, J. M., Massman, W. J., Ewers, B. E., & Williams, D. G. (2019). Bayesian analyses of 17 winters of water vapor fluxes show bark beetles reduce sublimation. *Water Resources Research*, *55*, 1598–1623. https://doi.org/10.1029/2018WR023054

Received 3 APR 2018
Accepted 12 DEC 2018
Accepted article online 17 DEC 2018
Published online 27 FEB 2019

Abstract Sublimation is an important hydrological flux in cold, snow-dominated ecosystems. In high-elevation spruce-fir forests of western North America, spruce beetle outbreaks have killed trees, reduced the canopy, and altered processes that control sublimation. We evaluated two hypotheses related to effects of disturbance on sublimation in this ecosystem: (1) the dominant source for sublimation is canopy intercepted snow and (2) the loss of canopy following a beetle disturbance leads to less total sublimation. To incorporate uncertainty hierarchically across multiple data sources and address phenomenological parsimony, Bayesian statistics were used to analyze 17 years (2000–2016) of winter eddy covariance flux data at the Glacier Lakes Ecosystem Experiments Sites AmeriFlux sites where a spruce beetle outbreak caused 75–85% basal area mortality. Our analysis revealed that resistances to sublimate snow from the canopy were an order of magnitude less than from the snowpack, and the maximum snow loading capacity in disturbed canopies was reduced to 34% of its pre-outbreak value. Total sublimation has decreased since 2010, 2 years after the main outbreak, declining 24% (with a 95% credible interval, C.I., between 18% and 38%) during 2014–2016 due to a 32% decrease in canopy sublimation. Snowpack sublimation only increased 3% over this period. With less total sublimation, the forest retained 6.1% (4.5–12.3% C.I.) more snowpack mass or equivalently 4.4% (3.2–8.8 C.I.) of the annual precipitation. Considering tree growth and ecological succession are slow in spruce-fir forests, this decrease in sublimation should persist as an increased snowpack for decades, with substantial impacts on catchment hydrologic processes and potentially streamflow.

1. Introduction

Sublimation is an important process in the water cycles of cold, snow-dominated land surfaces. It can account for the loss of a large portion of snowfall during the winter months and contributes a significant amount to annual water vapor fluxes (Kattelmann & Elder, 1991; Strasser et al., 2008). The amount of sublimation loss to the atmosphere during winter can be within an order of magnitude of the amount of soil water that is lost during other seasons through streams or into the ground water (Musselman, 1994; Schlaepfer et al., 2014). The importance of sublimation has been studied worldwide (Essery et al., 2003; Helgason & Pomeroy, 2011; Hiemstra et al., 2006; Kattelmann & Elder, 1991; MacClune et al., 2003; Molotch et al., 2007; Reba et al., 2012; Zhang et al., 2004; Zhang et al., 2008). Sublimation can account for half of the annual water vapor flux in subalpine forests of the central U.S. Rocky Mountains (Schlaepfer et al., 2014). Over the past decade, extensive spruce beetle outbreaks in many North American high-elevation spruce-fir forests have caused widespread tree mortality, led to needle loss, which opened up the canopy, and potentially altered the processes that control sublimation (Frank et al., 2014; Raffa et al., 2008).

Numerous snow process models have been developed for water forecasting (Rutter et al., 2009). Sublimation in these models is generally formulated as an extension of the Penman (1948) equation as a function of radiation, vapor pressure deficit, and turbulence, from one (Mahrt & Vickers, 2005; Pomeroy et al., 1998; Pomeroy et al., 2007) or two sources (Kongoli et al., 2014), or using an Ohm's law or Fick's law approach (Andreadis et al., 2009; Gelfan et al., 2004; Mahat et al., 2013; Yamazaki, 2001). These models use varying degrees of complexity to represent canopy interception of snow from forest characteristics such as leaf area, canopy closure, and gap area (Moeser et al., 2016; Pomeroy et al., 1998). In general, feedback between canopy interception and canopy sublimation is implicit in closing the canopy energy and mass balances (Mahat & Tarboton, 2014). Historically, sublimation and interception were measured by weighing lysimeters or tree-weighing devices (Schmidt, 1991; Storck et al., 2002; Suzuki & Nakai, 2008). The advent of eddy covariance measurements has allowed near continuous multiyear observations of sublimation, which can be analyzed to quantify cumulative trends (Molotch et al., 2007; Suzuki & Nakai, 2008) and to relate sublimation to its environmental drivers (Knowles et al., 2012). Eddy covariance data are often used to validate sublimation values predicted by process models evaluated around the world: in Arizona and New Mexico (Broxton et al., 2015; Svoma, 2017), Idaho (Kongoli et al., 2014), Colorado (Mahat et al., 2013; Marks et al., 2008; Sexstone et al., 2018), Wyoming (Chen et al., 2015), Canada (Pomeroy & Essery, 1999), France (Santaren et al., 2007), Tanzania (Cullen et al., 2007), and Tibet (Yang et al., 2011).

Snow models have been used to predict the hydrological response of forests to bark beetle disturbance. Conceptually, the loss of needles from the canopy and reduction of leaf area allows more (1) radiant energy, (2) wind, and (3) turbulence to penetrate the understory while (4) decreasing the canopy surface area to intercept snowfall such that (1)–(3) will increase sublimation throughout the ecosystem while (4) will decrease it from the canopy (Edburg et al., 2012; Pugh & Gordon, 2013). Modeling studies in Colorado and Wyoming have predicted less canopy sublimation and more water availability to the land surface following beetle disturbance (Chen et al., 2015; Livneh et al., 2015), while another in British Columbia predicted that the snowpack can contribute more sublimation than canopy intercepted snow (Bewley et al., 2010).

Observational studies have inferred different hydrological responses to bark beetles: accelerated snowmelt in Colorado based mainly on snowpack and radiation measurements (Pugh & Small, 2012); increased streamflow in Colorado identified by historical stream gauge measurements (Bethlahmy, 1974; Bethlahmy, 1975) or by using a water stable-isotope mass balance (Bearup et al., 2014); the potential for longer snowpack duration in Montana based mainly on snowpack and eddy covariance measurements (Welch et al., 2015); and minimal changes in Colorado and Wyoming based on streamflow, eddy covariance, stable-isotope measurements, and process models (Biederman, Harpold, et al., 2014; Biederman et al., 2015; Millar et al., 2017). There are few observational studies that investigate the sublimation response. In a Wyoming forest, the stable isotopes of snowpack were used to show that beetle impacted stands have higher sublimation (Biederman, Brooks, et al., 2014), but when eddy covariance data from that forest were compared to an unimpacted stand in Colorado, cumulative winter vapor loss was lower (Biederman, Harpold, et al., 2014). An analysis of the eddy covariance data from that Colorado site showed that the canopy contributes more sublimation than the snowpack (Molotch et al., 2007).

In this study, we analyzed 17 years of eddy covariance sublimation measurements from a subalpine spruce-fir forest severely disturbed by a spruce beetle outbreak (Figure 1). While a variety of statistical approaches could potentially be used to analyze these data, such as a time series analysis or a regression analysis relating sublimation to environmental drivers, these do not incorporate the physical processes that drive sublimation and thus cannot be used to explain or test hypotheses about the physical mechanisms of how bark beetles impact sublimation. By utilizing Bayesian statistics, our statistical model describes how sublimation is related to canopy interception, energy and snow mass balance, and environmental drivers using formulations similar to those found in snow process models while hierarchically incorporating uncertainty, providing probabilistic quantification of parameters, and penalizing overfitting with parsimony. This allows us to perform an analysis that not only quantifies the observed trends in sublimation, it provides insight into the underlying processes through which bark beetles cause these changes. We do not utilize snow process models (Rutter et al., 2009), which to our knowledge are all prognostic and not diagnostic. That is to say, they are predictive and do not fit parameters based on the probability that the snow process model fits the data. These are best used to evaluate hypothesis about how snow processes could respond under different scenarios, regardless of whether or not those scenarios actually occur. However, here our goal is to conduct a diagnostic analysis to evaluate hypotheses about how snow processes responded to a specific event that was observed. This requires us to implement a probabilistic feedback structure between parameters and data, which is not trivial to accomplish and requires some adaptation and simplification of snow processes in order to achieve statistical and computational stability. We use this analysis to evaluate the following hypotheses. (1) The mass of snow intercepted by the canopy is the dominant source of sublimation in a subalpine forest. (2) A spruce beetle outbreak, which causes substantial tree mortality, results in less canopy interception of snow and, thus, lower total sublimation from the ecosystem. We test these

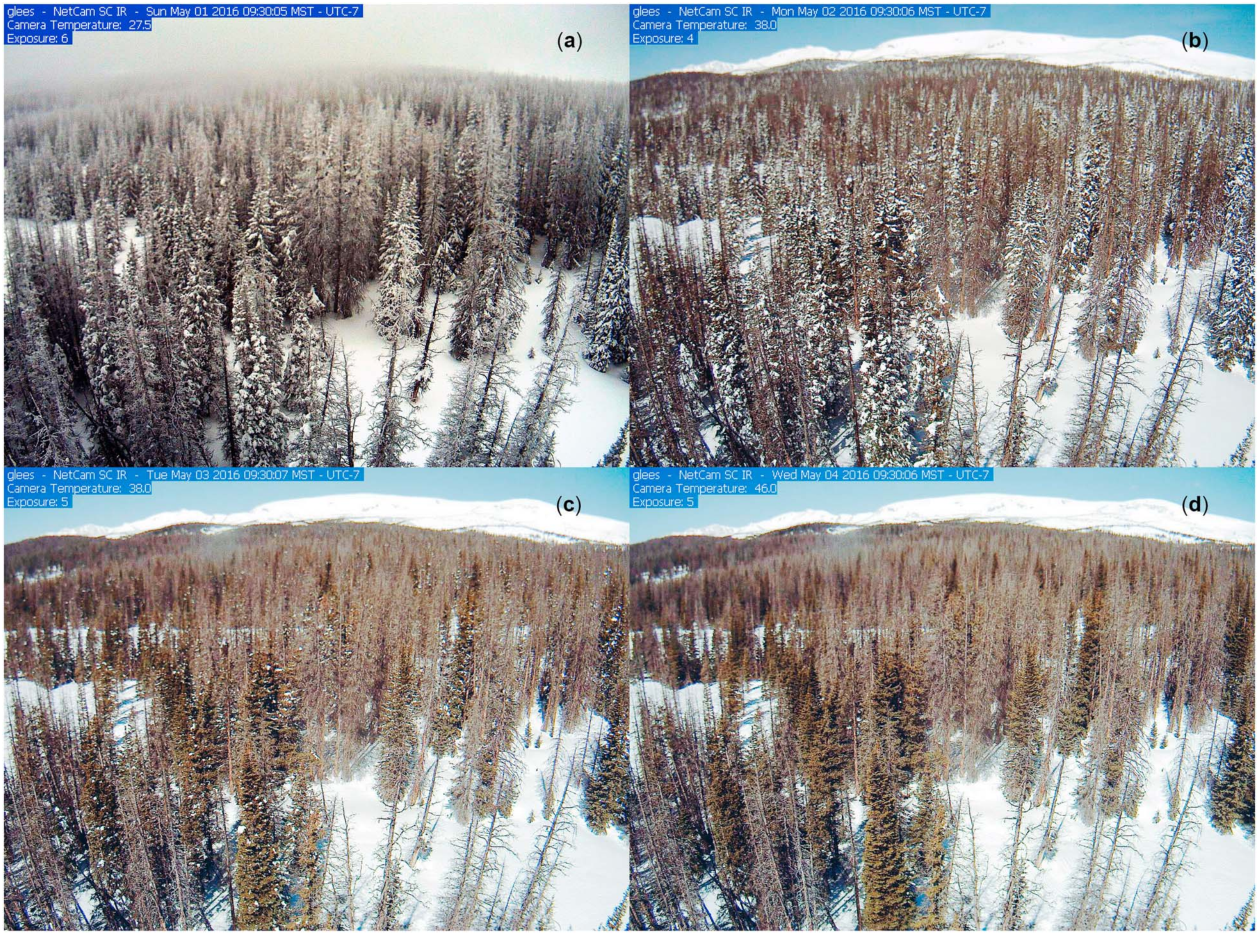

Figure 1. A snowstorm, which (a) fell on 1 May 2016 at the Glacier Lakes Ecosystem Experiments Site AmeriFlux site (http://ameriflux.lbl.gov/), deposits snowfall in the canopy that sublimates away over (b) 24, (c) 48, and (d) 72 hr. A major spruce beetle (*Dendroctonus rufipennis*) outbreak in this subalpine forest has caused significant Engelmann spruce (*Picea engelmannii*) mortality where the remaining snags (visible in the bottom right corner of each panel) have little ability to intercept snow. Photos courtesy of the Phenocam network (http://phenocam.sr.unh.edu).

hypotheses by comparing Bayesian posterior distributions that describe canopy versus snowpack sublimation based on forested leaf area observed with and without the impact of beetles.

2. Methods

2.1. Site Description

We examine the consequences of a spruce beetle (*Dendroctonus rufipennis*) epidemic on the winter sublimation of snow in an Engelmann spruce (*Picea engelmannii*)-subalpine fir (*Abies lasiocarpa*) forest in the Snowy Range mountains of southeastern Wyoming. The Glacier Lakes Ecosystem Experiments Site (GLEES) is a high-elevation forest (3,190 m) managed for long-term research by the Forest Service, U.S. Department of Agriculture since the 1980s (Musselman, 1994). Eddy covariance measurements have been conducted continuously for nearly two decades at the GLEES Brooklyn Tower (US-GBT, 1999–2006) and GLEES (US-GLE, 2004 to present) AmeriFlux sites (http://ameriflux.lbl.gov/). Beginning in the mid-2000s, a spruce beetle outbreak led to the mortality of a vast majority of mature spruce, reaching epidemic proportions in 2008 and causing widespread mortality in 2010 (Frank et al., 2014). As a consequence, 75–85% of the forested basal area had been affected (Fornwalt and Negron, unpublished data from 2010; Speckman et al., 2015). Here we consider data only from November to April, a timeframe that always has a persistent snowpack and is nearly always below freezing (Schlaepfer et al., 2014).

2.2. Measurements

2.2.1. Micrometeorology

A majority of the field measurements in this study come from the GLEES AmeriFlux site (41°21′59.55″N, 106°14′23.87″W). Eddy covariance fluxes of sensible heat (H, W/m^2) and latent heat (λE_s, W/m^2) between the land surface and the atmosphere were measured with a sonic anemometer (model SATI/3Vx, Applied Technologies, Inc., Longmont, CO, USA) and an open-path infrared gas analyzer (IRGA; LI-7500, Li-Cor, Inc., Lincoln, NE, USA) mounted at the height $z_a = 22.65$ m with the data processed each half-hour, median despiked (Frank et al., 2014), screened for quality assurance/quality control (QA/QC; Vickers & Mahrt, 1997), IRGA postcalibrated (Meek et al., 1998), rotated into planar-fit coordinates (Lee et al., 2004), time lag adjusted, spectrally corrected (Massman, 2000), and Webb-Pearman-Leuning corrected (Webb et al., 1980; including a modified version of the IRGA self-heating adjustment; Burba et al., 2008). One detail not relevant in Frank et al. (2014) was the use of a different IRGA from January to March 2006 (NIRGA, NOAA, Air Resources Laboratory, Atmospheric Turbulence and Diffusion Division, Oak Ridge, TN, USA). Wind velocity (U_a, m/s) and friction velocity (u_*, m/s) were also measured with the sonic anemometer. Ambient meteorological measurements were made of temperature (T_a, °C, RTD-810, Omega Engineering, Inc., Stamford, CT, USA), relative humidity (RH, %, 083D, Met One Instruments, Inc., Grants Pass, OR, USA), pressure (p_a, kPa, AB-2AX Intellisensor II, Atmospheric Instrumentation Research, Inc., Boulder, CO, USA and 61202 V, R. M. Young Company, Traverse City, MI, USA), four-component net radiation (R_n, W/m^2, which includes upwelling and net longwave radiation, $R_l\uparrow$ and $R_{n,l}$, respectively, PSP and PIR, Eppley Laboratory, Newport, RI, USA), and R_n (Q*5.571 Net Radiometer, Radiation and Energy Balance Systems, Inc., Bellevue, WA, USA). Further details are explained in Frank et al. (2014).

We present data from the GLEES Brooklyn Tower AmeriFlux site located 85 m south-southeast of the GLEES scaffold (41°21′56.82″N, 106°14′22.81″W), which was operational from November 1999 to August 2006 (http://ameriflux.lbl.gov/). The eddy covariance system was mounted due west at the height $z_a = 27.12$ m and featured a sonic anemometer (model SATI/3Vx, Applied Technologies, Inc., from November 1999 to January 2006) and three fast-response hygrometers: a NIRGA (NOAA, Air Resources Laboratory, Atmospheric Turbulence and Diffusion Division, from November 1999 to September 2002, September 2003 to March 2005, and August 2005 to January 2006, mounted 0.22 m east, 0.05 m north, and 0.25 m below the sonic), a LI-7500 (Li-Cor, Inc., from November 2001 to April 2002 and June 2002 to October 2003, mounted 0.29 m east, 0.19 m north, and 0.03 m above the sonic), and a KH2O (Campbell Scientific, Inc., Logan, UT, USA, from November 1999 to November 2001, mounted 0.14 m east, 0.08 m south, and 0.15 m below the sonic). The eddy covariance data were processed the same as the primary GLEES AmeriFlux data described above and in Frank et al. (2014) but required a different formulation of the self-heating correction appropriate for the NIRGA (Burba et al., 2008) and the oxygen correction for the KH2O (van Dijk et al., 2003). Ambient meteorological measurements were made of T_a and RH (CS500, Campbell Scientific, Inc., mounted at 27.8 m), p_a (AB-2AX Intellisensor II, Atmospheric Instrumentation Research, Inc., mounted at 27.4 m), four-component R_n (PSP and PIR, Eppley Laboratory, Newport, RI, USA, until September 2003, mounted at 28.7 m), and R_n (Q*5.571 Net Radiometer, Radiation and Energy Balance Systems, Inc., mounted at 28.7 m). Snowpack depth (z_p, m) was measured continuously at 3.12 m on this tower (Depth Sensor, Judd Communications, from July 2001 to June 2014 and January 2015 to present). We calculated values for vapor pressure deficit (D, kPa), density of dry air (ρ_d, mol/m^3), and density of water vapor (ρ_v, mol/m^3) above the land surface based on the meteorological measurements for both of the AmeriFlux sites.

We also present data from a subcanopy eddy covariance system mounted close to the snowpack at 6.5 m on the GLEES scaffold, which was installed in October 2012 and is available from the GLEES AmeriFlux site (http://ameriflux.lbl.gov/). Understory fluxes of latent and sensible heat sourced from the snowpack ($\lambda E_{s,p}$ and H_p, W/m^2) were measured with a sonic anemometer (model SATI/3Vx, Applied Technologies, Inc.) and an IRGA (LI-7500, Li-Cor, Inc.) on a boom pointed due west and extending ~1 m past the foliage of a mature subalpine fir, with the IRGA mounted 0.24 m east, 0.08 m south, and at the same height of the sonic. The eddy covariance data were processed the same as the primary GLEES AmeriFlux data described above and in Frank et al. (2014). Beginning in February 2014, four component net radiation was also measured above the snowpack (R_n^p, W/m^2, which includes net longwave radiation, $R_{n,l}^p$, CNR 4 Net Radiometer, Kipp & Zonen, Delft, The Netherlands). These data were screened to remove measurements concurrent with snow accumulation on the net radiometer.

2.2.2. Precipitation

Precipitation (P, mm snow water equivalent, SWE, converted to mol/m^2 for the statistical model) was measured at the nearby National Atmospheric Deposition Program (http://nadp.slh.wisc.edu/) site WY95 (41°21′53.57″N, 106°14′26.80″W) located 196 m south-southwest of the GLEES scaffold (Universal rain gauge, daily cumulative precipitation only, Belfort Instrument, Baltimore, MD, USA, until November 2008 and NOAH IV, ETI Instrument Systems, Fort Collins, CO, USA, November 2008 to present, both gauges shielded and unheated).

2.2.3. Gap Filling

For most ambient meteorological values surrogate data were available from other comparable measurement at the GLEES site (i.e., T_a, RH, p_a, U_a, R_n, and P and their calculated measurements D, ρ_d, and ρ_v). The z_p was gap filled with a simple model where height is incremented with new precipitation, which is assumed to exponentially decay from a snow density of 10% to 40% over 3 days of settling. The u_* was gap filled from a linear regression with U_a that was applied seasonally. From 2000 to 2016, 34%, 10%, 17%, 32%, 38%, 23%, 29%, 12%, 20%, 19%, 21%, 48%, 22%, 21%, 24%, 34%, and 42% of the winter λE_s data were missing. These were gap filled only to report cumulative sublimation; missing data were replaced with the values derived from our Bayesian analysis in section 2.4.

2.3. Modeled Predictor Variables

Several variables that we did not measure are required for the statistical analysis described in section 2.4. We estimated these values from various data sources available for our site. The methodologies used to model each of these predictor variables are described in the following sections.

2.3.1. Leaf Area Index

We characterized the change in one-sided leaf area index (LAI, m^2/m^2) over nearly two decades resulting from the spruce beetle outbreak by modeling the Moderate Resolution Imaging Spectroradiometer (MODIS) TERRA platform LAI (Myneni et al., 2002; https://lpdaac.usgs.gov/data_access, maintained by the NASA Land Processes Distributed Active Archive Center (LP DAAC), USGS/Earth Resources Observation and Science (EROS) Center, Sioux Falls, South Dakota, 2016) in the 1-km^2 pixel containing the AmeriFlux scaffold. Similar to Frank et al. (2014), the MODIS data were selected for peak summer LAI and screened for QA/QC; here we did not apply the coniferous forest multiplier of 2 for two-sided LAI appropriate for studies of gas exchange. We used a Bayesian analysis (Kruschke, 2014) to describe every MODIS measurement as $\mathrm{LAI} \sim N\left(\widehat{\mathrm{LAI}}, \sigma_\mathrm{LAI}\right)$ where the normal distribution is defined as $\theta \sim N(a, b)$ with expected value $E(\theta) = a$ and variance $\mathrm{var}(\theta) = b^2$. The predicted $\widehat{\mathrm{LAI}}$ is defined as a function of time (t_d, days) by the logistic sigmoid function

$$\widehat{\mathrm{LAI}} = \Delta_\mathrm{LAI} \tanh \frac{\beta_{50}(t_d - t_{50})}{\Delta_\mathrm{LAI}} + \mathrm{LAI}_{50} \tag{1}$$

where LAI_{50}, t_{50}, and β_{50} are process parameters for the LAI, time, and change in slope at the midpoint of the decline and Δ_LAI is the absolute change from the midpoint to the asymptote; all were defined with normally distributed prior distributions except σ_LAI, which had a gamma prior distribution. We define the pre-beetle LAI as the value at the left horizontal asymptote, which is $\Delta_\mathrm{LAI} + \mathrm{LAI}_{50}$. In situ radiation measurements of LAI collected from before the spruce beetle outbreak in an area of ~0.15 km^2 with ~10% overlap with the MODIS pixel and during the outbreak in the area of the eddy covariance measurement footprint (Nikolov & Zeller, 2006, Text S1 and Figure S1 in the supporting information) were compared to these MODIS based values.

2.3.2. Net Radiation Above the Snowpack

Net radiation above the snowpack was modeled because (1) the net radiometer at 6.5 m was not installed until February 2014 and (2) understory shortwave radiation measured with a single subcanopy radiometer often differs wildly from a more representative spatial average (Musselman et al., 2015). R_n^p is defined by

Beer's law with a canopy extinction coefficient (κ, unitless), which is assumed to apply equally to shortwave and longwave radiation (Ross, 1975; equation (2)).

$$R_n^p = e^{-\kappa \mathrm{LAI}} R_n \tag{2}$$

The value for κ was determined using Bayesian analysis. Only longwave measurements, $R_{n,l}$ and $R_{n,l}^p$, were used to estimate κ because of the uncertainty in understory shortwave measurements. Data were screened for QA/QC to remove measurements coincident with snow accumulation on the sensors. The Bayesian analysis described every half-hour measurement as $R_{n,l} \sim N\left(\widehat{R}_{n,l}, \sigma_{R_n}\right)$ and $R_{n,l}^p \sim N\left(\widehat{R}_{n,l}^p, e^{-\kappa \mathrm{LAI}} \sigma_{R_n}\right)$ where the process parameters $\widehat{R}_{n,l}$ were defined with uniform prior distributions, the values $\widehat{R}_{n,l}^p = e^{-\kappa \mathrm{LAI}} \widehat{R}_{n,l}$, κ and σ_{R_n} were defined with prior gamma distributions, and multiplying the standard deviation σ_{R_n} by Beer's law transmittance controlled for heteroscedasticity of residual errors caused by the different magnitudes of the radiation measurements.

2.3.3. Heat Flux Into the Snowpack

The heat flux into the snowpack (G, W/m^2) was modeled from an analysis that combined a snow accumulation and compaction model with a numerical solution to the heat equation using the explicit finite difference method. In short, snowpack density is a function of time and depth and was calculated from a Bayesian analysis of daily precipitation, snowpack height, and periodic snow pit measurements of vertical density profiles (Berryman et al., 2018). Thermal conductivity of snow was predicted from its density (Sturm et al., 1997). Finally, the heat equation was solved numerically assuming an upper boundary condition for snow temperature equal to the black body temperature associated with upwelling longwave radiation ($R_l\uparrow$) and a lower boundary condition of 0 °C.

2.3.4. Rate Change of Energy Stored in the Canopy

The rate of change of energy stored in the canopy (J, W/m^2) was a summation of the sensible and latent heat storage fluxes into the canopy airspace and the heat storage fluxes into the canopy leaves and trunks. Each component was estimated assuming a multilayer cylindrical canopy using the methodology of Haverd et al. (2007) and adapted for GLEES using site-specific forest inventories (Bradford et al., 2008; Fornwalt, unpublished data from 2010), allometrics and thermal properties for Engelmann spruce and subalpine fir (Kaufmann et al., 1982; Kaufmann & Troendle, 1981; TenWolde et al., 1988), and changes in trunk moisture content following spruce mortality (Laurila & Lauhanen, 2010). This term neglects the change in energy storage in the canopy snow as the amount of snow mass cannot be determined a priori to the Bayesian analysis. Considering that this mass will always be far less than the snowpack, its energy storage was assumed to be negligible relative to G.

2.4. Statistical Analysis

We analyzed 17 years of half-hour above canopy sublimation data, including 4 years with subcanopy eddy covariance measurements, to test hypotheses about the relative importance of the canopy and the impact of the beetle outbreak on sublimation. To accomplish this we used Bayesian statistics, which are implemented using Markov chain Monte Carlo (MCMC) methods (Kruschke, 2014). This approach allows us to explicitly define the likelihood of observing all of these data with a statistical model based on the two-source energy balance and canopy snow mass balance framework defined in the following sections. In a Bayesian framework, process parameters are assumed to have prior probability distributions, which are combined with the likelihood of observing the data to construct posterior probability distributions. A powerful property of Bayesian analysis is equivariance, where variables that are calculated from posterior parameters also have posterior probability distributions from which statistical inferences can be made; these are identified as derived quantities (Hobbs & Hooten, 2015). Therefore, while the Bayesian analysis directly estimates posterior distributions that define specific components of the conceptual framework (Figure 2), we can derive quantities that also have testable posterior distributions but are more recognizable (e.g., canopy snow mass, sublimation from the different sources, and interception with or without the impact of beetles). While Bayesian analysis can be similar to a frequentist analysis that uses maximum likelihood to estimate parameters, Bayesian techniques allow for more complex statistical models that are less correlative and more mechanistic or process based (Dormann et al., 2012). For example, in this study a time series analysis of sublimation data could demonstrate

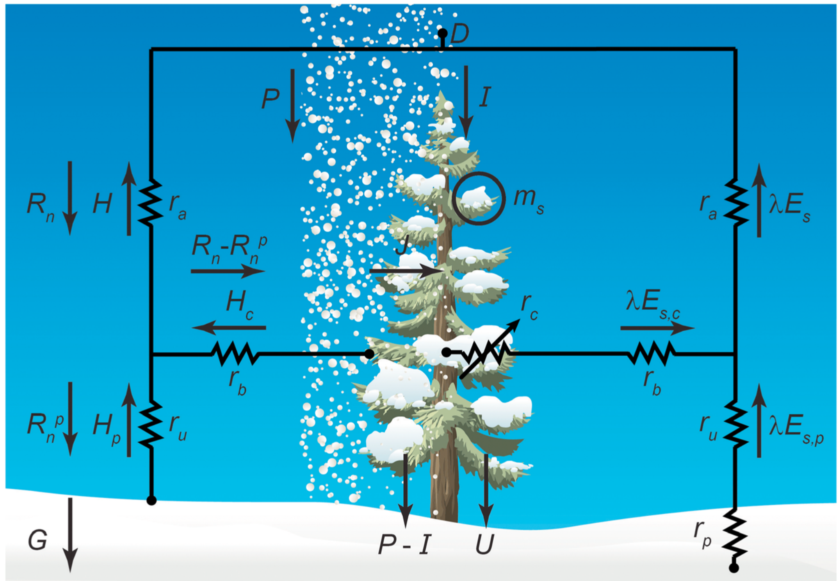

Figure 2. Conceptual diagram of the two-source energy balance and conservation of canopy snow mass framework used for statistical analysis of sublimation data. The canopy interception (I) of precipitation (P) is stored as mass in the canopy (m_s). Net radiation from above the land surface (R_n) and above the snowpack (R_n^p), heat flux into the snowpack (G), the rate change of energy stored in the canopy (J), and the vapor pressure deficit above the land surface (D) drive sensible (H) and latent heat flux (λE_s, i.e., sublimation) from the snowpack (p) and the canopy (c). These two paths of atmospheric resistance (r) restrict water vapor flow out of the snowpack and canopy, restrict heat and vapor flow through the understory (u) and canopy boundary layer (b), and aerodynamically resist (r_a) the turbulent fluxes as they ascend out of the land surface. When $E_{s,c}$ and canopy unloading (U) have depleted m_s below a threshold, then $r_c \to \infty$, transforming the system to a single source of sublimation from the snowpack.

a decreasing trend, though it could not take into account interannual climate variability; or a linear regression between sublimation and its environmental drivers could show a beetle mortality effect, though it could not explain or be used to test the processes causing this decline. A Bayesian analysis can address these shortcomings while also propagating uncertainties of the measurements and model structure through the analyses. Yet as MCMC techniques become more commonly applied to process-based models, it can be difficult to distinguish the difference between statistical analysis and stochastic simulation (Hartig et al., 2011). While our analysis is distinct from a forward (i.e., mechanistic) process model where no parameters are fitted, it can appear somewhat similar to a fitted process-based model where some parameters are fitted or tuned to a subset of data (Dormann et al., 2012). A Bayesian analysis is not an elaborate tuning exercise, but rather, the parameters are determined probabilistically as the most likely given the data and statistical model. The fundamental difference is the likelihood, which is calculated from the data for a statistical analysis but must be simulated for a stochastic simulation (Hartig et al., 2011). Thus, to some degree, the underlying processes described in a statistical analysis are implied by the data. A directed acyclic graph (Hobbs & Hooten, 2015) of the statistical model is presented in Figure 3.

2.4.1. Statistical Model: Two-Source Energy Balance Framework

In the Bayesian analysis, the likelihood is constructed from a data model describing every half-hour measurement of λE_s as a normal distribution defined with a mean ($\lambda\widehat{E}_s$) and standard deviation (process parameter σ, W/m^2; equation (3)).

$$\lambda E_s \sim N\left(\lambda\widehat{E}_s, \sigma\right) \tag{3}$$

The predicted mean ($\lambda\widehat{E}_s$) is derived from the sum of sublimation originating from two sources: snow intercepted by the canopy and the snowpack. To describe this process we adapt the two-component framework of Shuttleworth and Wallace (1985; Figure 2). This begins with the land surface energy balance

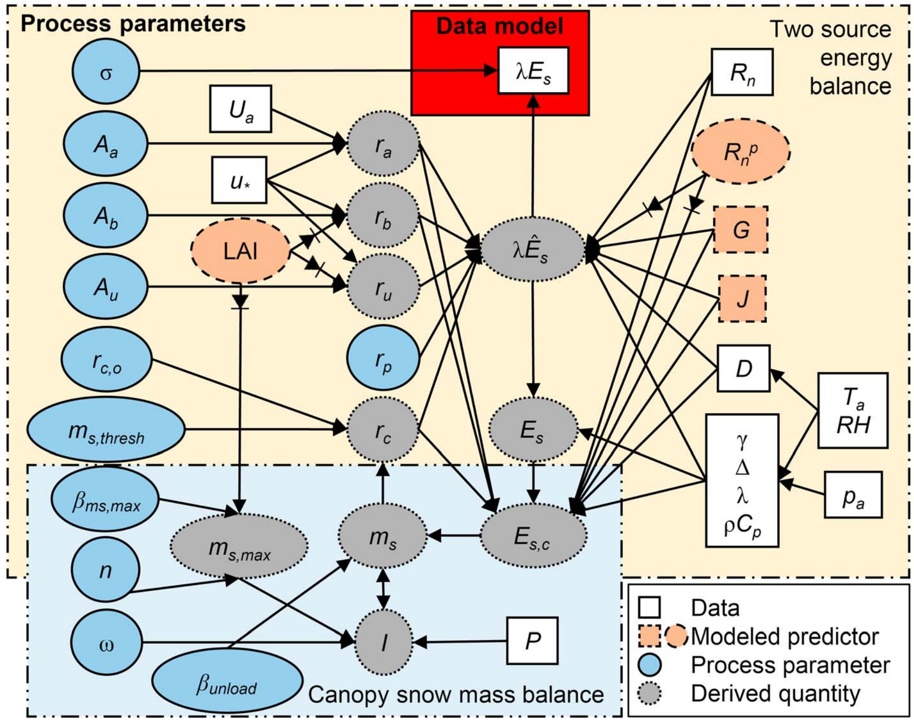

Figure 3. Directed acyclic graph conceptualizing the statistical analysis of sublimation data from 17 winters (2000–2016) at Glacier Lakes Ecosystem Experiments Site. The Bayesian data model fits latent heat flux measurements (λE_s) from a normal distribution with a predicted mean ($\lambda \widehat{E}_s$) based on the two-source energy balance and canopy snow mass balance. The Bayesian analysis combines micrometeorological data (white boxes), predictors that are modeled from the site (orange dashed boxes and ellipses), process parameters (blue ellipses) and derived quantities (gray dotted ellipses) to predict half-hourly data. The Bayesian analysis defines all process parameters with prior distributions and uses Markov chain Monte Carlo techniques to estimate their posterior distributions. Values within boxes are fixed throughout the analysis while those within ellipses have probability distributions. The Bayesian cut function (solid black diode symbol) restricts the flow of information in one direction between values with probability distributions. LAI = leaf area index.

$$H + \lambda E_s = R_n - G - J \tag{4}$$

This energy balance neglects, most notably, the horizontal advection of energy, which cannot be measured by eddy covariance. Using techniques similar to Penman (1948), latent heat flux can be defined as

$$\lambda \widehat{E}_s = \frac{\Delta\left[\left(a_3 \frac{r_a}{r_{b|u}} + a_1 + 1\right)(R_n - J) + (a_2 - a_1)R_n^p - \left(a_3 \frac{r_a}{r_{b|u}} + a_2 + 1\right)G\right] + a_3 \frac{\rho C_p}{r_{b|u}} D}{(\Delta + \gamma)\left(1 + a_1 + a_2 + a_1 a_2 + a_3 \frac{r_a}{r_{b|u}}\right)} \tag{5}$$

Latent heat flux from the land surface is constituted from the enthalpy of sublimation or vaporization (λ, J/mol; see equation (15)) and the sublimation of water vapor (E_s, mm SWE, converted to mol·m^{-2}·s^{-1} for the statistical model). Sublimation is driven by the net radiation above the land surface (R_n) and the snowpack (R_n^p), the heat flux into the snowpack (G), the rate change of energy stored in the canopy (J), and the vapor pressure deficit above the land surface (D). Aerodynamic resistance (r_a, s/m), canopy boundary layer resistance (r_b, s/m), canopy snow resistance to water vapor flow (r_c, s/m), snowpack resistance to water vapor flow (r_p, s/m), and understory resistance (r_u, s/m) are defined below (see equations (11)–(14)). The slope of the saturation vapor pressure to air temperature (Δ, kPa/K), density of air (ρ, kg/m^3), specific heat of air (C_p, J·kg^{-1}·K^{-1}), and psychrometric constant (γ, kPa/K) are defined below (see equations (16)–(18)). The parallel resistance $r_{b|u}$ is defined as

$$\frac{1}{r_{b|u}} = \frac{1}{r_b} + \frac{1}{r_u} \tag{6}$$

Finally, ratios a_1 through a_3 are defined as

$$a_1 = \frac{\gamma r_p}{(\Delta + \gamma) r_u} \tag{7}$$

$$a_2 = \frac{\gamma r_c}{(\Delta + \gamma) r_b} \tag{8}$$

$$a_3 = 1 + \frac{\gamma (r_c + r_p)}{(\Delta + \gamma)(r_b + r_u)} \tag{9}$$

Once all snow sublimates from the canopy (Figure 1), we consider the forest to be a dual sensible heat/single latent heat sourced system. The framework from Massman (1992) can be adapted to describe the process when the snowpack becomes the only source of sublimation (equation (10)).

$$\lambda \widehat{E}_s = \frac{\Delta\left(\frac{r_a}{r_a + r_u}(R_n - J) + \frac{r_u}{r_a + r_u} R_n^p - G\right) + \frac{\rho C_p}{r_a + r_u} D}{\Delta + \gamma\left(1 + \frac{r_p}{r_a + r_u}\right)} \tag{10}$$

The fundamental difference between the two-source versus one-source sublimation framework is the canopy snow resistance to water vapor flow, such that as $r_c \rightarrow \infty$ then equation (5) converges to equation (10). Thus, r_c is defined toward an asymptotic resistance (process parameter $r_{c,o}$, s/m) for ample snow but approaches infinity when the mass of snow within the canopy (m_s, mm SWE, converted to mol/m^2 for the statistical model) sublimates below a threshold (process parameter $m_{s,\mathrm{thresh}}$, mol·s m^{-3}; equation (11)).

$$r_c = r_{c,o} + \frac{m_{s,\mathrm{thresh}}}{m_s} \tag{11}$$

By defining r_c in this manner, the statistical model essentially transitions between one and two sources of water.

We define the other resistances in our statistical model through phenomenological relationships to their important environmental drivers. Aerodynamic resistance (r_a) is adapted from Brutsaert (1982) from the wind velocity and friction velocity above the land surface (equation (12)).

$$r_a = A_a \frac{U_a}{u_*^2} \tag{12}$$

We modified the definition in Brutsaert (1982) to include the process parameter (A_a) because an argument can be made that due to imperfect measurements of latent energy (i.e., the potential for surface energy imbalance) that all resistances in the two-source framework should be fit to the data, and we used model selection, that is, parsimony, analysis (Spiegelhalter et al., 2002) to justify this alteration (analysis not shown). Canopy boundary layer resistance (r_b) is defined as a reduced expression from Massman (1999) comprising LAI, u_*, and a process parameter (A_b) (equation (13))

$$r_b = \frac{A_b}{\left(1 - e^{-\frac{\mathrm{LAI}}{2}}\right)\sqrt{u_*}} \tag{13}$$

Snowpack resistance to water vapor flow (r_p) is a process parameter that is considered constant through time, though it probably changes dramatically with morphology of the snow surface, which varies between fresh powder and ice. Finally, understory resistance (r_u) is the series combination of within-canopy aerodynamic resistance and snowpack boundary layer resistance, which we define from the geometric mean of these from the formulations in Massman (2004) comprising LAI, u_*, and a process parameter (A_u) (equation (14))

$$r_u = A_u \sqrt{\mathrm{LAI}} u_*^{\frac{4}{3}} \tag{14}$$

Other definitions include

$$\frac{\lambda}{m_v} = \begin{cases} 2835, & T_a \leq 0^{\circ}\mathrm{C} \\ 2501 - 2.37T_a, & T_a > 0^{\circ}\mathrm{C} \end{cases} \tag{15}$$

$$\rho C_p = m_d \rho_d C_{p,d} + m_v \rho_v C_{p,v} \tag{16}$$

$$\Delta = 0.61365 \frac{(17.502)(240.97)}{(240.97 + T_a)^2} e^{\frac{17.502 T_a}{240.97 + T_a}} \tag{17}$$

$$\gamma = \frac{m_d C_p p_a}{\lambda} \tag{18}$$

which contain the specific heat of dry air ($C_{p,d}$ = 1010 J·kg^{-1}·K^{-1}), specific heat of water vapor ($C_{p,v}$ = 1846 J·kg^{-1}·K^{-1}), molecular mass of water vapor (m_v = 18.0153 g/mol), and molecular mass of dry air (m_d = 28.9625 g/mol).

2.4.2. Statistical Model: Canopy Snow Mass Balance

A canopy snow mass balance that receives input from canopy intercepted precipitation (I, mol/m^2) and loses output as snow unloading (U, mol/m^2) and canopy sublimation ($E_{s,c}$, mm SWE, converted to mol·m^{-2}·s^{-1} for the statistical model) is included in the statistical model. For consecutive half hours, t and $t + 1$, this is calculated as

$$m_s(t+1) = m_s(t) + I(t) - U(t) - \int E_{s,c}(t)\mathrm{d}t \tag{19}$$

We use the canopy interception model of Hedstrom and Pomeroy (1998) (equation (20))

$$I = \left(m_{s,\max} - m_s\right)\left(1 - e^{-\frac{\omega P}{m_{s,\max}}}\right) \tag{20}$$

where the maximum snow load in the canopy ($m_{s,\max}$, mm SWE, converted to mol/m^2 for the statistical model) is a function of LAI and ω is a process parameter related to the area of canopy coverage per area of ground, which is a simplification from Hedstrom and Pomeroy (1998). We defined $m_{s,\max} = \beta_{ms,\max}$ LAI^n where $\beta_{ms,\max}$ (mol/m^2) and n are process parameters. This is a modification from Hedstrom and Pomeroy (1998) where the exponent allows a stronger relationship between changes in LAI and the maximum snow loading; we used model selection analysis (Spiegelhalter et al., 2002) to justify this alteration (analysis not shown). While it is possible that ω should also decrease following the outbreak, we set it constant for computational simplicity and justify this because most of the dead trees remain standing as snags with intact branches, which cover roughly the same projected surface area on the ground (Figure 1). The quantity $m_{s,\max}$ accounts for the fact that these trees have little snow load capacity. Unloading is defined as $U = m_s \beta_{\mathrm{unload}}$, which is similar to (Hedstrom & Pomeroy, 1998) by simply unloading a fixed proportion of canopy snow at all times; β_{unload} is a process parameter. To complete the canopy snow mass balance, the sublimation from the canopy is defined (equation (21)).

$$E_{s,c} = \frac{1}{\lambda} \frac{\Delta\left[\left(1 + \frac{r_a}{r_b}\right)(R_n - J) - R_n^p - \frac{r_a}{r_b} G\right] + \frac{\rho C_p}{r_b} D - (\Delta + \gamma)\frac{r_a}{r_b}\lambda E_s}{\Delta + \gamma\left(1 + \frac{r_c}{r_b}\right)} \tag{21}$$

The canopy snow mass neglects snowmelt (assumed to be negligible due to consistent below freezing temperatures) and the temperature dynamics of the maximum snow load (Hedstrom & Pomeroy, 1998).

2.4.3. Expanding the Data Model to Include Measurements of $\lambda E_{s,p}$, H, and H_p

We also considered measurements from the subcanopy eddy covariance system, which began in 2012, to enhance our understanding of how sublimation is partitioned. We conducted four data analyses covering the 2013–2016 water years with expanded data models to predict measurements of (I) λE_s, (II) λE_s and $\lambda E_{s,p}$, (III) λE_s and H, and (IV) λE_s, $\lambda E_{s,p}$, H, and H_p. Because these four analyses only considered postbeetle years when LAI had stabilized, the maximum snow loading was simplified to $m_{s,\max} = \beta_{ms,\max}$ LAI (i.e., the exponent n was removed from LAI). For these analyses, the likelihood is expanded to predict each half-hour measurement with $\lambda E_{s,p} \sim N\left(\lambda \widehat{E}_{s,p}, \sigma\right)$, $H \sim N\left(\widehat{H}, \sigma\right)$, and $H_p \sim N\left(\widehat{H}_p, \sigma\right)$ using the predicted quantities for latent and sensible heat in equations (22)–(24).

10.1029/2018WR023054

$$\lambda\widehat{E}_{s,p} = \lambda\widehat{E}_s - \lambda E_{s,c} \tag{22}$$

$$\widehat{H} = R_n - G - J - \lambda\widehat{E}_s \tag{23}$$

$$\widehat{H}_p = R_n^p - G - \lambda\widehat{E}_{s,p} \tag{24}$$

In analyses (III) and (IV), all of the energy balance terms in equation (4) are included as either data or modeled predictors. This can be an issue because of the well-known energy imbalance problem at flux sites (Stoy et al., 2013; Wilson et al., 2002). To avoid this, we applied separate energy balance closure process parameters ($\psi_{\lambda Es}$ and ψ_H) to fit the latent and sensible heat flux measurements and we used model selection analysis (Spiegelhalter et al., 2002) to justify separate parameters (analysis not shown).

2.4.4. Computation

We performed all analyses using R (version 3.2.2; R Core Team, 2015). To estimate the parameters describing the modeled predictors LAI and R_n^p (i.e., LAI_{50}, t_{50}, β_{50}, Δ_{LAI}, and $\varkappa$), we used packages CODA (Plummer et al., 2006) and rjags (Plummer, 2015b) within RStudio (version 0.99.486; RStudio Team, 2015) and implemented MCMC analysis with JAGS (version 4.0.0; Plummer, 2003). Because these modeled predictors are estimated with uncertainty that we desire to include in subsequent analyses, we used the Bayesian cut function, which allows the flow of information to go forward from one parameter to a second, but not backward from the second to the first (Plummer, 2015a). This forces (1) our estimate of LAI to incorporate the mean and standard deviation provided by the MODIS data product, (2) our estimate of the canopy extinction coefficient to incorporate the uncertainty in LAI, and (3) our statistical analyses of sublimation to take into account the uncertainties in LAI and R_n^p. Plummer (2015a) demonstrated that a parameter can be "cut" in an MCMC analysis by updating it only after the rest of the parameter set has been updated multiple times and allowed to converge; this forces the cut parameter to be weakly dependent on its previous value. An extreme case of this is to run multiple Bayesian analyses (i.e., iterations), each with a randomly sampled value for the cut parameter, which is fixed in the analysis, and then creating an ensemble MCMC chain (i.e., pooling) from the individual analyses/iterations (Plummer, 2011). We use this iterative approach to implement the cut function by randomly sampling the cut parameters from (1) the prior distribution of LAI based on the MODIS data product, (2) the posterior distribution of LAI from the analysis in section 2.3.1, and (3) the posterior distributions of LAI and R_n^p from the analyses in sections 2.3.1 and 2.3.2. To estimate LAI with the Bayesian cut function, we performed 1,000 iterations of (1) generating a dataset from the MODIS means/standard deviations and (2) running a single MCMC chain, which was adapted, burned in, and sampled over 100, 1,900, and 2,000 steps, respectively; the values for each process parameter at the final step of each iteration were pooled together to create the final cut posterior. To estimate $\varkappa$ with the Bayesian cut function, we performed 1,000 iterations of (1) sampling from the LAI posterior and (2) running a single MCMC chain, which was adapted, burned in, and sampled over 100 steps each. We used shorter chains because the $R_{n,l}$ and $R_{n,l}^p$ data sets were large and burn-in was achieved very rapidly. The final cut posterior for $\varkappa$ was merged with the four parameters for LAI to create a final MCMC chain with 1,000 samples.

We performed all statistical analyses of sublimation in R with a custom MCMC sampler using high-performance computing provided by the University of Wyoming (Advanced Research Computing Center, 2012). Each analysis was compiled from 1,000 iterations of the cut function that sampled the modeled predictors LAI and R_n^p. Each iteration was an independent 5,000-step MCMC analysis where burn-in was completed in ~500 steps. The final posterior distributions were compiled from the values of the process parameters at the final step of each iteration. For every process parameter we define a prior gamma or uniform distribution: A_a (gamma, expected value ± [variance]$^{0.5}$ = 1 ± 1), A_b (gamma, 10 ± 10), $r_{c,o}$ (gamma, 50 ± 50 s/m), $m_{s,\mathrm{thresh}}$ (gamma, 10 ± 10 mol·s·m^{-3}), r_p (gamma, 50 ± 50 s/m), A_u (gamma, 10 ± 10), $\beta_{ms,\max}$ (gamma, 10 ± 10 mol m^{-2}), n (gamma, 1 ± 1) and ω (uniform, between 0 and 1), β_{unload} (gamma, 0.0012 ± 0.0012), σ (gamma, 50 ± 50 W/m^2), $\psi_{\lambda Es}$ (gamma, 1 ± 1), and ψ_H (gamma, 1 ± 1). These prior distributions are generally noninformative and defined with plausible expected values. The only exception is the unloading parameter, which was given an expected value inspired by Hedstrom and Pomeroy (1998) of 0.0012 or 0.12% unloading per half hour, which is equivalent to 33% unloading per week. While several derived quantities are required to define the statistical model (equations (5)–(14) and (20)–(21), and Figure 3), others are calculated for the purpose of

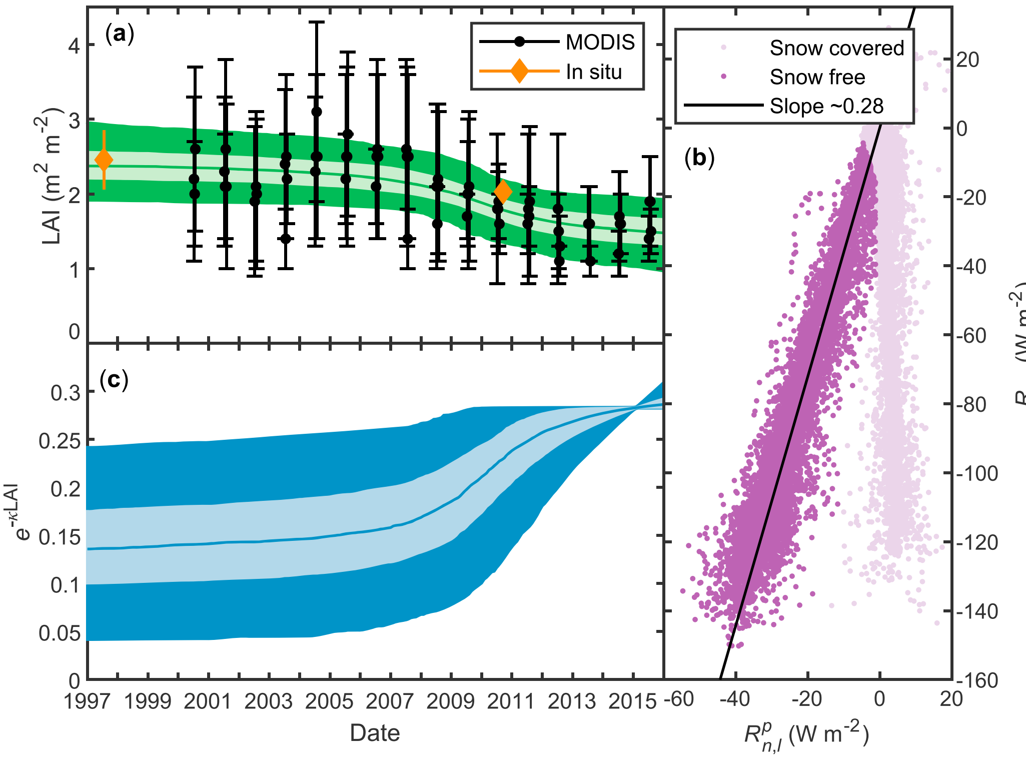

Figure 4. Two important drivers of the statistical model are the change in leaf area index, LAI, and Beer's law transmittance, $e^{-\kappa\text{LAI}}$, due to the spruce beetle epidemic. (a) The change in LAI was modeled with the Bayesian cut function (green shading) using the Moderate Resolution Imaging Spectroradiometer (MODIS) LAI data from the site (black dots with error bars). Average in situ LAI values measured in 1997 and 2010 (orange diamonds with error bars, Text S1) are within the 95% credible intervals. (b) Transmittance and the canopy extinction coefficient, κ, were determined from the relationship between net longwave radiation above the canopy ($R_{n,l}$) versus above the snowpack ($R^p_{n,l}$; purple dots) once data were screened for snow on the lower instrument (lighter shading). Sensors were installed above the snowpack in February 2014. (c) The posterior distributions for LAI and κ were combined to determine the posterior probability of $e^{-\kappa\text{LAI}}$ over time (blue shading). In (a) and (c), shading represents the median, inner quartile range, and 95% credible interval of the posterior distributions.

hypothesis testing; most notably the amount of sublimation assuming “no beetles,” which was achieved by setting LAI constant with the pre-beetle LAI value from each iteration of the cut function (Figure 4). We make statistical inferences between posterior probability distributions by comparing their 95% credible intervals (C.I.s; Lu et al., 2012); these are crucially different from confidence intervals in frequentist analyses, which assume an entire data set can be repeated (McElreath, 2016). When 95% C.I.s do not overlap, it can be interpreted as statistically “significant” in a manner similar, but more rigorous and justifiable than the traditional p-value where $p < 0.05$ (McElreath, 2016).

3. Results

3.1. Modeled Predictors LAI and R^p_n

LAI decreased and transmittance increased by roughly a factor of 2 during the spruce beetle outbreak (Figure 4). LAI decreased from the prebeetle LAI of 2.4 (with a 95% C.I. between 2.0 and 3.4) m^2/m^2 to 1.3 (0.4–1.8 C.I.) m^2/m^2 with a maximum change (β_{50}) of 0.153 (0.014–1.91 C.I.) m^2·m^{-2}·year^{-1} centered (t_{50}) in January 2010 (December 2007 to November 2011 C.I.). These parameters were highly correlated. The trend in LAI resulted in inner quartile ranges and 95% credible intervals that typically spanned 0.3 and 1 m^2/m^2 with a significant decrease over time (Figure 4a). Average values of in situ LAI measurements from before and during the beetle outbreak (2.46 ± 0.40 and 2.03 ± 0.12 m^2/m^2, mean ± standard error, Text S1) are not statistically different from this trend because these values are within the 95% credible intervals (Figure 4a). Our analysis of Beer's law was based on long-wave radiation measurements above and within the canopy from 2014 to 2016, when the transmittance, $e^{-\kappa \mathrm{LAI}}$, was ~0.28 (Figure 4b). This allowed us to estimate the canopy extinction coefficient, κ, as 0.84 (0.65–1.23 C.I.; a similar value of 0.98 ± 0.05 was found in a forest 15 years after a spruce budworm attack; Aubin et al., 2000), which was also highly correlated with the four parameters describing LAI. By sampling directly from this joint posterior distribution we retained the correlation between parameters and could estimate the trend in transmittance over time (Figure 4c). The transmittance increased from ~0.15 to ~0.28 during the beetle outbreak, with large uncertainty in the early years when the inner quartile range and 95% credible interval spanned ~0.08 and ~0.20 before becoming fairly certain in recent years when direct observations were available.

3.2. Analyzing the Impact of the Spruce Beetle Outbreak

In our analysis of 109,014 half-hour λE_s measurements from 17 winters (2000–2016), total ecosystem sublimation declined during the spruce beetle outbreak, falling by 24% (18–38% C.I.), which is equivalent to the amount of snow in 6.1% (4.5–12.3% C.I.) of the winter precipitation or 4.4% (3.2–8.8% C.I.) of the annual precipitation in the three most recent years. A time series plot of sublimation shows a decrease from 2011 to 2016, which corresponds to the postoutbreak years (Figure 5b), while a plot of sublimation versus precipitation shows that the slope of this relationship decreases in 2011–2016 (Figure 5c). The Bayesian analysis produced predictions of $\lambda \widehat{E}_s$ that were similar to observations on both annual (Figures 5b, 5c, and 6) and half-hour (Figures 7a and 8a) timescales. A qualitative "goodness of fit" estimate for the analysis is to compare the standard deviation of all observed λE_s (43 W/m^2) to the standard deviation of the model residual errors (30 W/m^2, Figure 9k and Table S2), which can roughly be interpreted as an R^2 ~ 0.5. For each process parameter the choice of prior distribution had virtually no influence on the posterior distribution (Figure 9). One parameter of note is β_{unload}, which was given a prior expected value of 0.12% unloading per half hour or 33% per week, but converged to a posterior distribution of 0.00020% per half hour or 0.07% per week. This analysis indicates that unloading was relatively inconsequential, possibly because the remarkable turbulence at GLEES (Frank et al., 2014) causes a vast majority of canopy intercepted snow to sublimate before it has the opportunity to unload.

The Bayesian cut function propagated uncertainty in LAI and R_n^p to the rest of the analysis by increasing the variance in each process parameter from within individual MCMC chains to between iterations. While this minimally affected $r_{c,o}$ and β_{unload}, this increased the standard deviation of the other parameters (Figures 9a and 9b, 9d–9i, and 9k) by at least 37–260%, with notable increases of 2,700% and 4,200% in parameters associated with canopy interception and interact directly with LAI ($\beta_{ms,\max}$ and n). Even though sensible heat flux measurements were not considered in the analysis, the underlying energy balance closure in the statistical model (equation (4)) led to derived quantities for H that were similar to the observations (Figures 7b and 8b). Snow load in the canopy is derived by accumulating precipitation while losing mass through sublimation and unloading (Figures 7c and 8c). The maximum snow load ($m_{s,\max}$) in the canopy decreased during the spruce beetle outbreak from 11.2 (8.9–86.6 C.I.) to 3.6 (0.0–5.0 C.I.) mm SWE. The source of sublimation rapidly switched between the canopy and snowpack (Figures 7d and 8d), though more total contribution came from the canopy (Figures 7e and 8e).

It is impossible to know what would have been observed had the spruce beetle epidemic not occurred. Instead, the predicted $\lambda \widehat{E}_s$ (i.e., "outbreak") can be compared to the values derived with LAI and R_n^p fixed to their pre-outbreak levels (i.e., no beetles). In this analysis, the outbreak resulted in significant reductions in sublimation beginning in 2010 (Figure 6). From 2010 to 2016 the spruce beetle outbreak decreased canopy sublimation (median of −17%, −25%, −25%, −24%, −32%, −33%, and − 32% by year), increased snowpack sublimation (median of 2%, 5%, 2%, 3%, 4%, 3%, and 4% by year), and decreased ecosystem sublimation (median of −12%, −22%, −17%, −18%, −25%, −23%, and − 25% by year; Figure 6 and Table S3). This translates to a reduction in sublimation equivalent to 3.4%, 4.4%, 4.8%, 5.1%, 6.0%, 6.1%, and 6.3% of the winter precipitation or 2.0%, 3.3%, 3.3%, 3.2%, 4.1%, 4.2%, and 4.9% of the annual precipitation (Figure 5a). The differences when quantities were derived with no beetles are shown in Figure 8, where more snow was intercepted into the canopy (Figure 8c), resulting in a

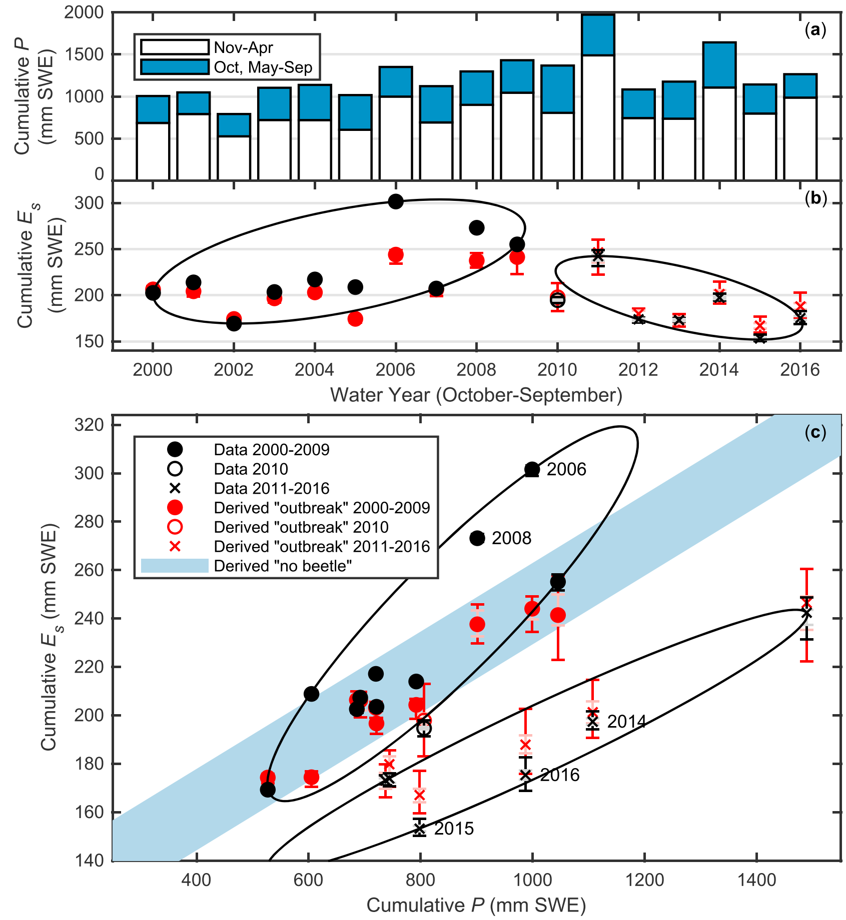

Figure 5. Seventeen years of observed (a) precipitation, P, and (b) sublimation, E_s, at Glacier Lakes Ecosystem Experiments Site (millimeters of snow water equivalent, i.e., SWE). A time series analysis of sublimation might show a significant trend following the beetle outbreak (2010–2016), though the effects of interannual climate variability would not be taken into consideration. (c) Winters with higher precipitation generally result in higher sublimation. This relationship is reduced following a spruce beetle outbreak, though a regression analysis would not explain the processes controlling this change. Results derived from the Bayesian analysis describing the "outbreak" (red shading) are similar to the observations with notable exceptions in 2006 and 2008. The light blue shading is a region enclosing each of the 17 years of sublimation derived from the Bayesian analysis describing "no beetles." Symbols and shaded error bars represent the median, inner quartile range, and 95% credible interval of the posterior distributions. Ellipses are the minimum areas that encircle the prebeetle (2000–2009) and postbeetle (2011–2016) observations. "Derived" quantities are calculated from posterior parameters and have posterior probability distributions from which statistical inferences can be made.

higher contribution from the canopy to the total (Figure 8d) and higher ecosystem sublimation rates (Figure 8e).

3.3. Expanding Bayesian Analyses to Include Subcanopy Turbulent Fluxes and Above Canopy Sensible Heat Flux

Our analysis was expanded to include subcanopy eddy covariance measurements from four winters (2013–2016). In the analysis of 21,800 half-hour measurements of $\lambda E_{s,p}$ along with 24,194 measurements of λE_s during the same timeframe, the cumulative contribution of the canopy to sublimation decreased from 68% to 57% (Figure S2); a simple comparison of observed $\lambda E_{s,p}$ to observed λE_s indicate this was 36%. It is possible, though, that the subcanopy eddy covariance measurements at 6.5 m were not purely sourced from the snowpack, but also contained sublimation from the canopy of small trees. Estimates for most process parameters changed including an increase in $r_{c,o}$ and decreases in $m_{s,\text{thresh}}$, r_p, and ω (differences in 95% credible intervals; Figure S3 and Table S2). The parameter β_{unload} increased

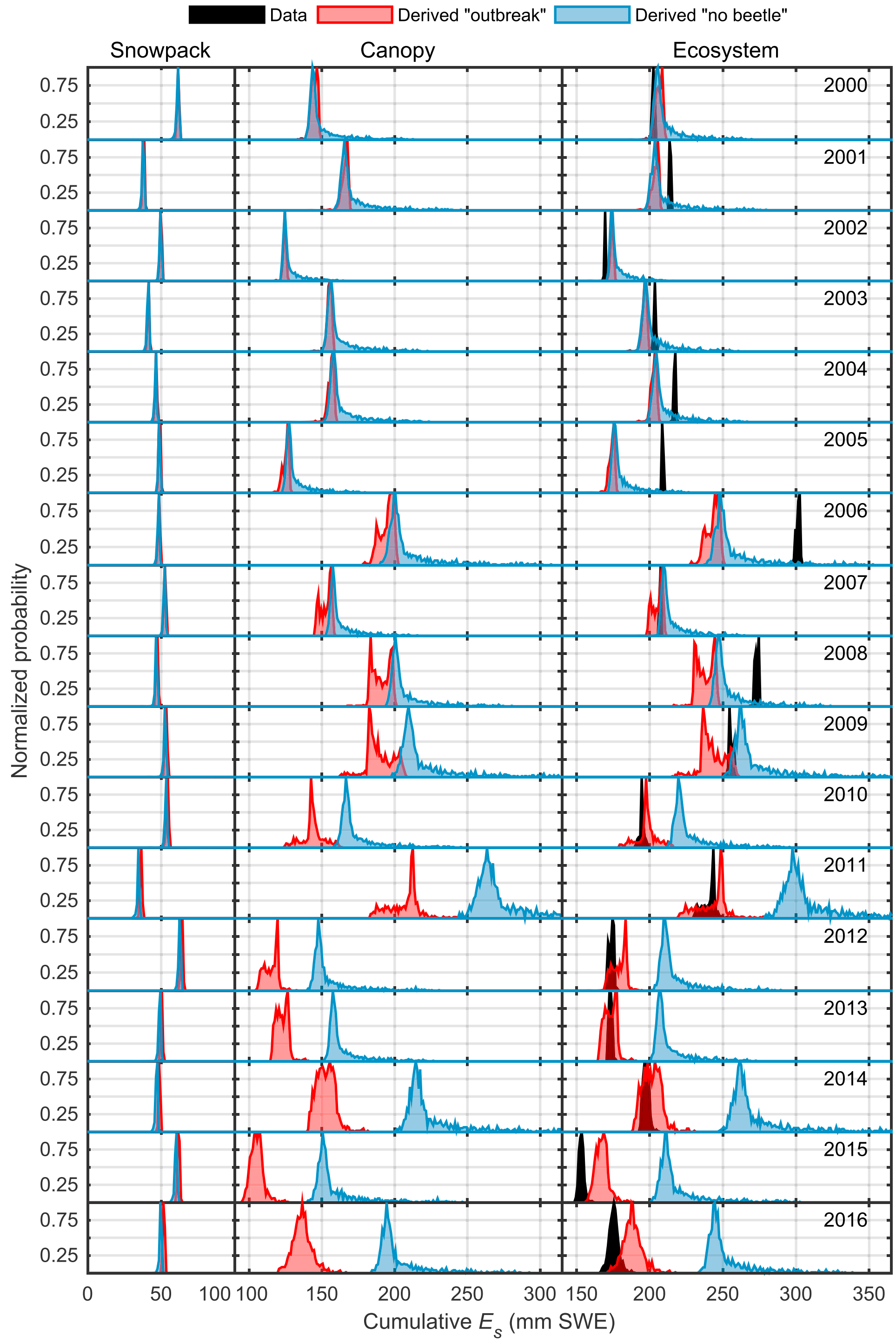

Figure 6. Results from the Bayesian analysis deriving sublimation (millimeter of snow water equivalent, i.e., SWE) from the snowpack, canopy, and ecosystem for 17 winters (2000–2016) at Glacier Lakes Ecosystem Experiments Site. Posterior distributions for sublimation were derived from (I) the observed decrease in leaf area index (LAI, Figure 3a) characterizing the beetle “outbreak” (red shading) versus (II) fixed LAI (i.e., “no beetles,” blue shading). As the outbreak progressed, there was a significant reduction in canopy sublimation relative to no beetles, which reduced total ecosystem sublimation. “Derived” quantities are calculated from posterior parameters and have posterior probability distributions from which statistical inferences can be made. The distributions for the observed data (black) are due to gap filling.

10.1029/2018WR023054

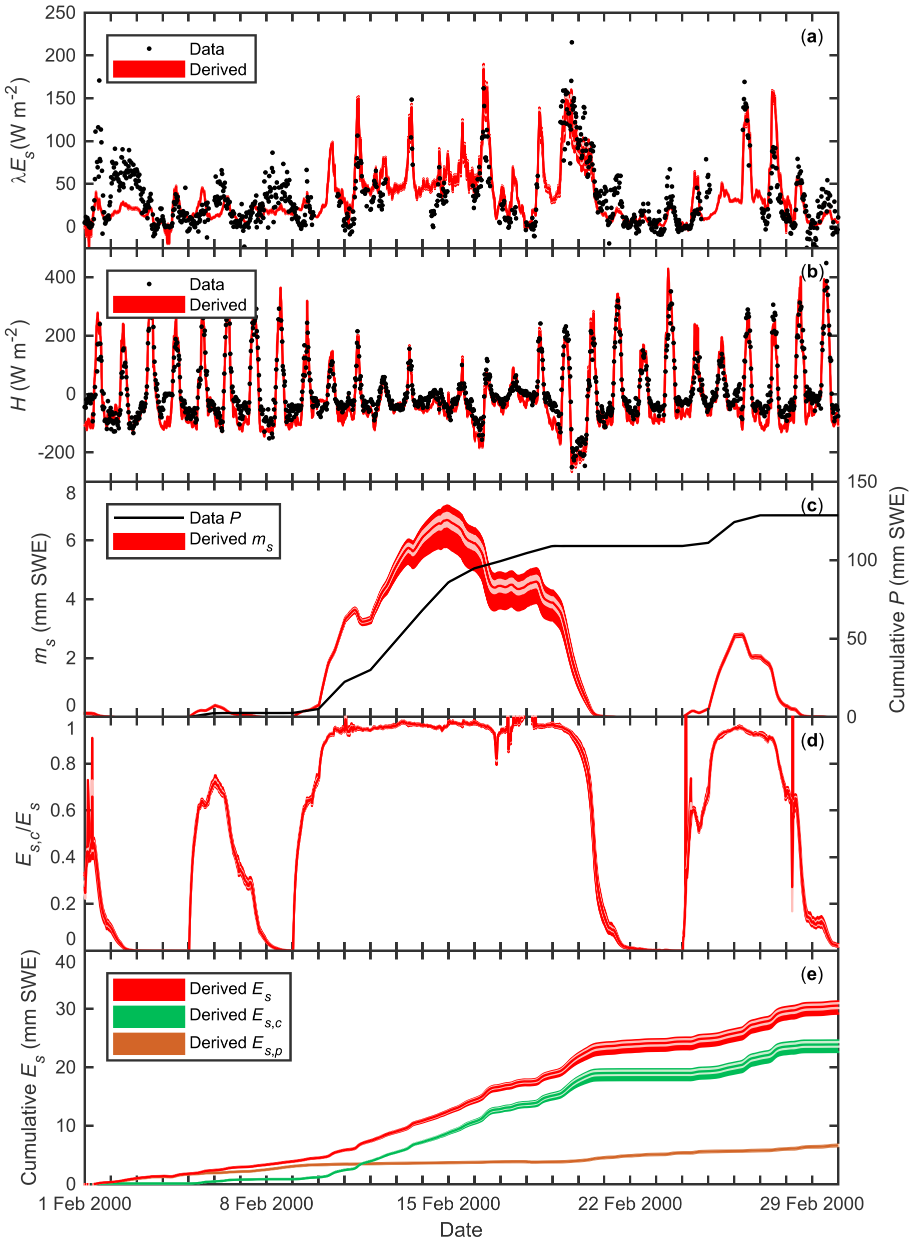

Figure 7. A 1 month excerpt before the beetle outbreak from the analysis of 17 years of (a) observed latent heat flux of sublimation (λE_s) data (black dots). A statistical model based on the two-source energy balance and canopy snow mass balance is used to derive predictions of λE_s (red shading). (b) Sensible heat flux (H) derived from the analysis (red shading) exhibits similar dynamics as observations (black dots, not used in the statistical model). (c) Cumulative precipitation (P, black line) is intercepted as a mass of snow within the canopy (m_s, red shading), which is depleted by canopy sublimation ($E_{s,c}$) and unloading. (d) Total ecosystem sublimation is sourced from the canopy the majority of time and (e) $E_{s,c}$ (green shading) accounts for a majority of total cumulative sublimation (red shading) while snowpack sublimation ($E_{s,p}$, brown shading) is a lesser contributor. "Derived" quantities are calculated from posterior parameters and have posterior probability distributions from which statistical inferences can be made. Data were collected at the Glacier Lakes Ecosystem Experiments Site-Brooklyn Tower AmeriFlux site. Shading represents the median, inner quartile range, and 95% credible interval of the posterior distribution for each derived quantity. Units presented as snow water equivalent (SWE).

only slightly to 0.40–0.50% unloading per week. While the values $\lambda\widehat{E}_s$ and $\lambda\widehat{E}_{s,p}$ derived from the analyses of one or two eddy covariance systems were not obviously different for any particular half-hour (Figures S4a and S4b), the main difference when including both systems was a reduced ability of the canopy to intercept snow (Figure S4c) and contribute to total sublimation (Figure S2).

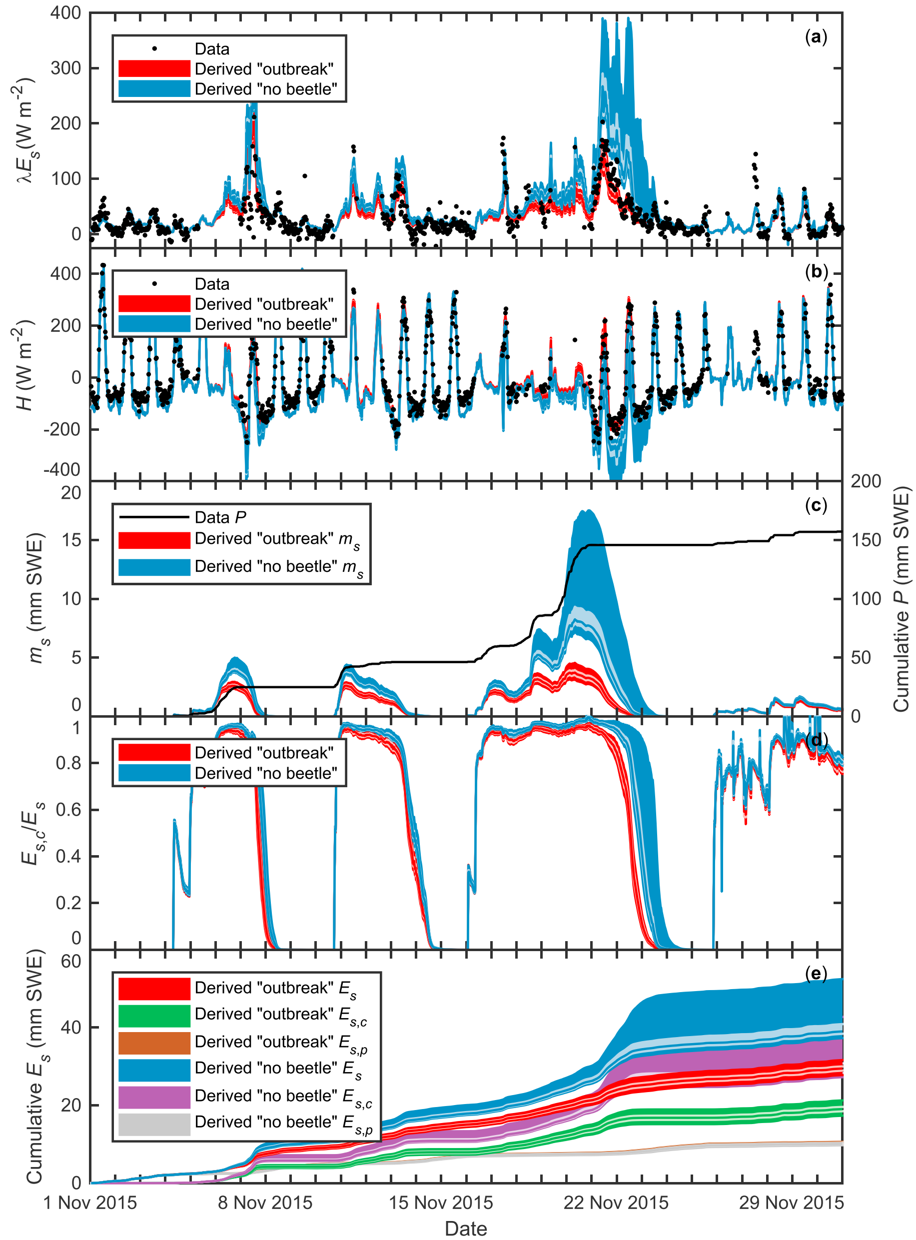

Figure 8. A 1 month excerpt after the beetle outbreak from the analysis of 17 years of (a) observed latent heat flux of sublimation (λE_s) data (black dots). Quantities were derived with (I) the observed decrease in leaf area index (LAI, Figure 3a) characterizing the beetle outbreak (red shading) versus (II) fixed LAI (i.e., "no beetles," blue shading). (b) Observed (black dots) and derived (red/blue shading) sensible heat flux (H). (c) Assuming no beetle impact, more precipitation (P, black line) is intercepted, resulting more mass of snow within the canopy (m_s, blue versus red shading), (d) a higher contribution of canopy sublimation ($E_{s,c}$) to total sublimation (blue versus red shading), and (e) more cumulative E_s (blue versus red shading) and $E_{s,c}$ (purple versus green shading) while snowpack sublimation ($E_{s,p}$) is mostly unchanged (gray versus underlying brown shading). "Derived" quantities are calculated from posterior parameters and have posterior probability distributions from which statistical inferences can be made. Data were collected at the Glacier Lakes Ecosystem Experiments Site AmeriFlux site. Shading represents the median, inner quartile range, and 95% credible interval of the posterior distribution for each derived quantity. Units presented as snow water equivalent (SWE).

When 24,194 half-hour measurements of H and 21,800 of H_p were included in the analysis, energy balance closure parameters for latent heat flux (7–10%, $\psi_{\lambda Es}$) and sensible heat flux (−16%, ψ_H) were required to fit the data (Figures S3k and S3l and Table S2). In these analyses the vapor source resistances, r_c and r_p, increased (e.g., combinations of $m_{s,\mathrm{thresh}}$, $r_{c,o}$, and ω, Figures S3c–S3e and S3i, and Table S2), while the

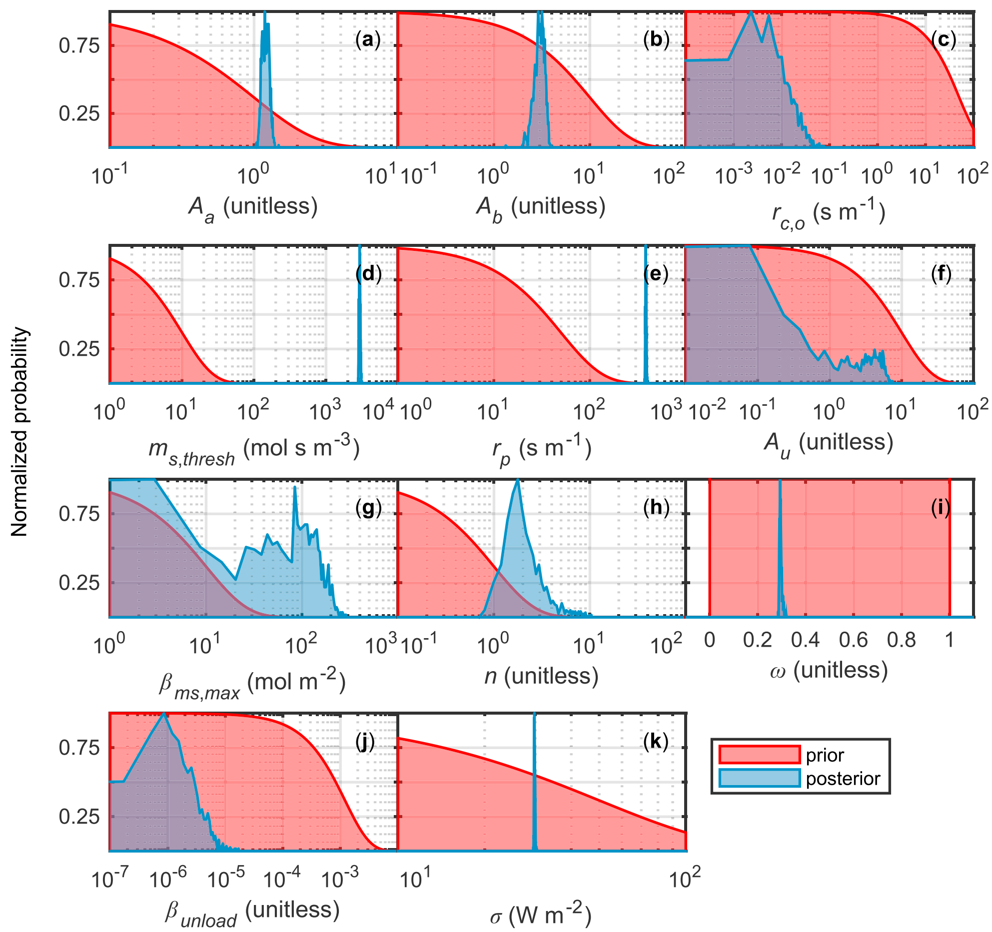

Figure 9. Prior (red shading) and posterior (blue shading) probability distributions of process parameters from the Bayesian analysis of 17 winters (2000–2016) at Glacier Lakes Ecosystem Experiments Site. (a) A_a, (b) A_b, (c) $r_{c,o}$ and (d) $m_{s,\text{thresh}}$, (e) r_p, and (f) A_u are parameters related to the aerodynamic resistance, canopy boundary layer resistance, canopy snow resistance to water vapor flow, snowpack resistance to water vapor flow, and understory resistance; (g) $\beta_{ms,\max}$, (h) n, and (i) ω are related to the canopy interception of snow; (j) β_{unload} is the half-hour unloading coefficient; and (k) σ is the standard deviation of the latent heat flux predictions. Most horizontal axes are plotted on a log scale.

boundary layer resistances, r_b and r_u, decreased (e.g., A_b and A_u, Figures S3b and S3f, and Table S2), which tended to promote the flow of sensible heat while restricting the release of vapor.

4. Discussion

We retain our hypothesis (1), that is, most sublimation originates from the canopy, by rejecting the alternative hypothesis (i.e., sourced from the snowpack) based on statistical analyses that estimated resistance pathways that facilitate a majority of latent energy flow from the canopy (Figure 9). We retain our hypothesis (2), that is, the spruce beetle outbreak decreased sublimation, by rejecting the alternative hypothesis (i.e., no change in sublimation) based on the analysis comparing the amount of sublimation derived from an intact canopy versus one with the observed decrease in LAI. In all years since 2010 there was a significant reduction in the cumulative sublimation from the canopy and the ecosystem (Figure 6).

4.1. Accounting for Data Uncertainty With the Bayesian Cut Function

Bayesian analysis provides a powerful tool for analyzing data with complex models while accounting for uncertainty in both data and statistical models (Gelman et al., 2014). Yet a practical issue is that it is often necessary to compartmentalize analyses and then convey the results from one into another. Typically, this is done through fixed values or as process parameters with prior probability distributions; neither are satisfactory as the former neglects uncertainty and the latter can lead to excessive shrinkage in the posterior distributions (Kruschke, 2014). In this situation shrinkage is not beneficial because the random variables being conveyed between analyses become more certain than originally indicated. Instead, the Bayesian cut function is a new tool where information flows between parameters much like through a check valve or diode, which facilities communication of "different data sets…via summary statistics" (Plummer, 2015b). Essentially, the cut function allows for parameter estimation at lower levels of a Bayesian hierarchy, which can then propagate upward and influence the rest of an analysis, without allowing the upper levels of the hierarchy to propagate downward and influence the parameter estimation. In our application, the cut function allows modeled predictors to be brought into the analysis via probability distributions, which describe their uncertainty and cannot be altered. While there is no consensus on how to implement the Bayesian cut function, Plummer (2015b) showed that this can be achieved during MCMC sampling by updating the cut parameter only after all other parameters are allowed to converge, or in the extreme case, by iteratively running the analysis using randomly generated data drawn from the prior parameter distribution to be cut (Plummer, 2011). In this study we used the cut function to allow (1) the uncertainty in MODIS data to flow into our analysis LAI, (2) the uncertainty in LAI to flow into our analysis of Beer's law transmittance, and (3) the uncertainty in LAI and R_n^p to flow into the analysis of sublimation (Figure 3). In the analysis of 17 years of sublimation data the cut function forced more variability into all process parameters (especially those related to the interception of snow), yet sublimation derived from the pack, canopy, and the ecosystem was still fairly constrained (Figures 6, 7e, and 8e) and revealed clear and significant trends due to the beetle outbreak. To our knowledge, this study is a novel application of incorporating data uncertainty in the statistical analysis of micrometeorological data interacting with water vapor from the Earth's surface.

4.2. The Process of Sublimation

Based on the results from our Bayesian analysis, we retain our first hypothesis that in a high-elevation spruce-fir forest, sublimation predominantly originates from the canopy. This is regardless of whether the forest has a full canopy or has been severely affected by a spruce beetle outbreak (Figures 6, 7d and 7e, and 8d and 8e). Even our most conservative result, obtained after massive forest mortality and with direct measurements of snowpack sublimation, shows that the canopy is a major contributor to the total ecosystem sublimation (Figure S2). As long as a reasonable amount of snow is present in the canopy, the resistance network in our conceptual framework (Figure 2) favors canopy sublimation; the analysis estimates small atmospheric and canopy resistances (median r_a, r_b, and r_c range between 5 and 23 s/m, derived from Figures 9a–9d with r_c evaluated for >1 mm SWE in the canopy) against large snowpack resistances (median $r_p = 383$ s/m, Table S2). The inverse Stanton number, B^{-1} (expressed as kB^{-1} with k being the vonKarman constant), associated with canopy boundary layer resistance was estimated as 1.7 (0.6–2.8 C.I.) which is relatively small and likely associated with a large heat transfer coefficient in the canopy (Massman, 1999). This explains why the system abruptly switches between snowpack and canopy (Figures 7d and 8d): snow in the canopy is extremely easy to sublimate while snow in the pack is not (Nakai et al., 1999). Because the canopy distributes snow three dimensionally (Pomeroy & Schmidt, 1993), it provides more surface area and less resistance for sublimation than the snowpack, which is essentially a two dimensional surface. Canopy snow sublimates away within a few days in the absence of new snowfall (Figures 1, 7c, and 8c), which is consistent with observations in Saskatchewan, Canada (Hedstrom & Pomeroy, 1998). Following the outbreak at our site, we estimate that between one half and two thirds of all sublimation originates from the canopy (Figures 6 and S1, and Table S3) and that the bigger the snow year, for example, 2011 and 2014 (Figure 5a), the more the canopy dominates the total balance (Figures 6 and S1). A similar trend was observed at Niwot Ridge, Colorado, USA, where 55% of all sublimation originates from the canopy and the energy balance favors substantial canopy sublimation following snowstorms (Molotch et al., 2007). There are similarities in the ability to predict sublimation at these two sites: our Bayesian analysis derived predictions of sublimation with an $R^2 \sim 0.5$, whereas at Niwot Ridge an energy balance snowmelt model predicted latent energy with a correlation of 0.54 ($R^2 \sim 0.3$; Mahat et al., 2013). Another study used a different process-based snow model to predict daily sublimation from this site with an R^2 of 0.30 (Sexstone et al., 2018). An interpretation of our results is that canopy sublimation occurs at the expense of snowpack sublimation. This is consistent with the difference in the proportion of snow accumulation that is sublimated away from an exposed snowpack (16–41%) versus an enclosed one (4–8%) in a study conducted in Idaho, USA (Reba et al., 2012).

These results are inferred from a Bayesian analysis based on the two-source framework of Shuttleworth and Wallace (1985). A more common approach to identify the sources of water vapor is with stable isotopes (Good et al., 2012; Noone et al., 2011, 2013; Williams et al., 2004). We measured water vapor isotopic concentrations on the tower from 2014 to 2016 but were unable to improve our ability to partition sublimation between the canopy and snowpack because of difficulties in accurately measuring isotopic concentrations of canopy sublimation (Text S2). In this study, a process based Bayesian analysis that explains sublimation data was more effective at identifying the different sources of water than could be determined by concurrent and continuous stable isotope of water vapor measurements.

Our Bayesian analysis could not accurately predict both λE_s and H data without adding parameters that account for a surface energy imbalance in the measurements. We found that measurements of H were 16% smaller than values derived from equations (23) and (24), while measurements of λE_s were 7–10% higher than derived from equations (5) and (22) (Figures S3k and S3l). Part of the explanation for the imbalance in H could be our use of ATI sonic anemometers, which Frank et al. (2016) found could underestimate all fluxes by 3–4%, though this is in opposition to the overestimate in λE_s. Some of the imbalance could also relate to errors in measuring available energy, of which we have observed that different instruments measure different R_n at our site (9% difference in slope between Eppley and Radiation and Energy Balance Systems measurements observed in the US-GLE data set, $R^2 = 0.99$). A portion of the H imbalance could be due to the advection of sensible heat, which was neglected from our energy balance and can be sizeable in a coniferous forest (Moderow et al., 2007). Finally, we mention that while G and J were relatively small (root-mean-square values of 2.6 and 12.8 W/m^2, respectively, compared to 183.5 W/m^2 for R_n) they had to be modeled at our site. The energy imbalance problem has stumped researchers at flux sites for decades (Leuning et al., 2012; Stoy et al., 2013; Wilson et al., 2002) and our winter imbalance at GLEES is no exception and is comparable to the 0.77 found at nearby Niwot Ridge, Colorado (Mahat et al., 2013). But our results do offer some insights. The closure coefficients for λE_s and H are in opposite directions from unity, meaning if a problem lies within the eddy covariance measurements then it might not be a general error in the technique (i.e., turbulence measurements or processing) but rather something that impacts these two measurements differently (i.e., temperature versus vapor instrumentation). Since the magnitude of λE_s is much less than H during the winter (Figures 7a versus 7b, 8a versus 8b) more emphasis should probably be put on the H imbalance, which is similar to the finding of Helgason and Pomeroy (2012) over a snowpack in Saskatchewan, Canada. This differs from the more conventional assumption that the Bowen ratio determined from eddy covariance measurements is correct and that H and λE_s are underestimated in similar proportions (Twine et al., 2000).

4.3. The Impact of Spruce Beetle Outbreak on Ecosystem Sublimation

By comparing sublimation values derived from the beetle-caused decrease in LAI relative to fixed LAI (i.e., no beetles) that were produced from analysis of 17 years of half-hour sublimation data at GLEES, we retain our second hypothesis that total ecosystem sublimation decreased following a spruce beetle outbreak. This trend can be illustrated qualitatively through a time series (Figure 5b) or by comparing the relationship between the observed precipitation and sublimation before and after 2010 (Figure 5c), the year of peak tree mortality and LAI decrease (Frank et al., 2014). Quantifying the beetle impact with these types of analyses is difficult because sublimation is not a simple function of time, precipitation, or any other variable. Bayesian techniques enable data analysis based on conceptual frameworks and processes; in this application sublimation can be related to precipitation, temperature, humidity, wind, net radiation, and leaf area (Figure 3) through the processes and equations often found in deterministic, first principles-derived, snow models. A statistical model based on two-source energy balance and canopy snow mass balance framework performs well at predicting the observations at both half-hour (Figures 7a, 8a, and 9k) and seasonal (Figures 5b and 5c, and 6) timescales. Through this analysis we can quantify the impact of outbreak by deriving sublimation with and without the observed beetle impact on forest structure. By doing this, we detected a significant difference in sublimation as early as 2010 (difference in 95% credible intervals, Figure 6), 2 years after a significant decline in growing season ET could be found (Frank et al., 2014).

Considering that canopy sublimation is dominant in our ecosystem, results indicated that the spruce beetle outbreak caused the maximum snow capacity of the canopy to decrease to 34% of the pre-epidemic values (derived from Figures 9g and 9h). Comparing results derived with and without the beetle impact on LAI, the change in $m_{s,\max}$ led to an obvious impact on the water balance. When the forest catches less snow in the canopy then it sublimates less snow from the ecosystem. In the last three winters this led to 32% less canopy sublimation (Figure 6). There was a modest 3% increase in snowpack sublimation (Figure 6), which is a response similar to a nearby lodgepole pine (*Pinus contorta*) forest impacted by mountain pine beetle (*Dendroctonus ponderosae*; Biederman, Brooks, et al., 2014). Snowpack observations following a canopy replacing fire also suggest that snowpack sublimation can increase following disturbance (Harpold et al., 2014) and canopy sublimation increases with leaf area from forest management practices (Koeniger et al., 2008). The combination of these is 24% less total sublimation from the ecosystem, which is equivalent to 6.1% of the total winter precipitation or 4.4% of the annual input (Figure 6). There is some consistency between this and a recent study by Sexstone et al. (2018) who predicted the impact of spruce beetle and mountain pine beetle on sublimation in a high-elevation 3,600-km^2 study area along the continental divide 136 km south-southeast from GLEES. The results of their process-based, deterministic snow model implied that sublimation could decrease 7% from the canopy, increase 9% from the surface, and decrease in total 4% across the landscape. Though the total amount of decrease we observed was nearly 1 order of magnitude larger, only 11% of their study was classified with a high leaf area mortality similar to what was observed at GLEES. Even though it was a different forest type, the field site in Biederman, Brooks, et al. (2014) was nearby to ours, being 35 km south-southeast and 435 m lower in elevation. The contrast between their results, which indicate sublimation increased following mountain pine beetle, and ours, which indicate it decreased following spruce beetle, demonstrates the delicate balance between radiant energy, wind, turbulence, and canopy surface area in the conceptual response of sublimation to beetles (Edburg et al., 2012; Pugh & Gordon, 2013).

Water is important in semiarid regions of western North America and a reduction in sublimation equivalent to ~6% more snowfall retained by the snowpack is a hydrologically, ecologically, and socially meaningful increase for consumptive uses, which is principally crop irrigation in Wyoming and the North Platte drainage of Nebraska (Jacobs & Brosz, 1993; Shinker et al., 2010). We estimate the 95% credible interval of the reduction in sublimation to be equivalent to 5–12% of the snowpack, which is a similar range to the desired increase in snowfall of 5–15% set by a weather modification experiment pilot study in the mountains of southeastern Wyoming (the US-GBT AmeriFlux site was a target area in this study) to test the feasibility and economic impact of orographic cloud seeding (Breed et al., 2014; Wyoming Water Development Commission, 2014). Schlaepfer et al. (2014) showed that at GLEES, roughly half of all precipitation returns back to the atmosphere as water vapor, and roughly half of that is in the form of sublimation. In other high-elevation forests in the Rocky Mountains, sublimation from a persistent snowpack can exceed incoming precipitation over the course of a month (Molotch et al., 2007). Though sublimation rates are relatively low at GLEES and account for roughly one quarter of the incoming snowfall, winter lasts a long time. Though our analysis was limited to November–April, it is not uncommon to find snow at this site well into July. In this context, 24% less total sublimation due to the spruce beetle outbreak takes on more importance. Frank et al. (2014) found that summer evapotranspiration also decreased 28–36% at GLEES due to the spruce beetle outbreak. The ramifications of this are that for at least the 9 months of the year covered by these studies, this ecosystem retains more water after the outbreak than it did before. This accounts for all but the shoulder seasons, of which spring is modeled at GLEES to produce more runoff and earlier snowmelt (Chen et al., 2015). Taken together, it is reasonable to expect that more water was available in this ecosystem in the years following the peak mortality, which is consistent with the observed increase in soil moisture (Frank et al., 2014). It is uncertain how long the reductions in growing season evapotranspiration will continue as the understory plants respond (Boucher & Mead, 2006; Millar et al., 2017), postbeetle increases in soil moisture lessen (Norton et al., 2015), and the surviving trees have a growth release (Veblen et al., 1991). Since the sublimation process is intimately tied to the canopy, at least the winter change in ecosystem water balance should persist for decades while forest succession begins in the understory (Aplet et al., 1988).

There has been debate whether or not bark beetle outbreaks lead to increased streamflow from impacted forests. Conceptually, this could be expected (Gray & Andersen, 2009; Troendle & King, 1985) and some observational studies support this (Bearup et al., 2014; Bethlahmy, 1974), while others suggest there is minimal change (Biederman, Harpold, et al., 2014; Biederman et al., 2015). Hillslope water budgets from a watershed in the transition between spruce-fir and lodgepole forest 3.4 km away and 240 m downhill to the southeast of

GLEES show that the majority of water from the melting snow pack drains past the root zone and thus is not dramatically impacted by the decline in tree transpiration after bark beetle mortality (Thayer et al., 2018). The results from our analysis are consistent with the increased streamflow observed following a spruce beetle outbreak in a spruce-fir forest in Bethlahmy (1975) but they cannot firmly support one notion or the other, especially with regard to higher order streams and rivers further down the watershed. This is not simply because we do not present data for the entire annual hydrological cycle. The subalpine spruce-fir forest where our site resides is perched above lower elevation mixed conifer forests that have been impacted by mountain pine beetle. Any water that leaves our forest must travel at least 500 m downhill and over 7 km through different forests, which are likewise recovering from disturbance (Biederman, Brooks, et al., 2014; Biederman, Harpold, et al., 2014; Reed et al., 2014), in order to reach the high plains of Wyoming. If the spruce-fir forests do produce more streamflow, the ultimate fate of that water is currently unknown.

5. Conclusion

We analyzed the impact of a spruce beetle outbreak on sublimation in a high-elevation spruce-fir forest over 17 years of observations. A spruce beetle outbreak at the GLEES AmeriFlux sites caused 75–85% basal area mortality and dramatically reduced leaf area. Following the loss of canopy, the forest could only intercept a third of the mass of snow as it could prior to the outbreak. This is consequential because the resistance to sublimate snow from the canopy is an order of magnitude less than from the snowpack, which means canopy sublimation is favored as long as that mass is available. In the past few years, the loss of canopy has increased the available energy transmitted to the snowpack and led to a modest 3% increase in sublimation from this source. But the overwhelming loss of intercepted snow has led to 32% less canopy sublimation and ultimately 24% less sublimation from the ecosystem. This is equivalent to 6.1% of the snowfall or 4.4% of the total annual precipitation being retained in the snowpack. When taken in conjunction with studies investigating the impact of the outbreak during other seasons at this site, it is reasonable to expect that a sizeable amount of water is no longer utilized in this forest. We demonstrated that with Bayesian statistics, an analysis of sublimation data can be conducted with relatively complex statistical models that resemble the functional relationships found in snow process models but with the ability to incorporate uncertainty in the models and data. This broadens the capacity of the analysis to go beyond just substantiating that changes occurred in this spruce-fir forest over 17 years, but to provide insight into the processes through which bark beetles decreased sublimation.

Acknowledgments

We thank Jared Baker for his assistance with the Mount Moran high-performance computer. We thank John Korfmacher, Kate Dwire, Bob Musselman, and Alan Ellsworth for countless years of help and expertise at GLEES. We thank Karl Zeller and Don Hazlett for the 1997 GLEES LAI data and Roberto Bazan, Kate Dwire, and Paula Fornwalt for the 2010 GLEES LAI data. We thank Bob Hall, Shannon Kay, and reviewers associated with Water Resources Research (Editor Jessica Lundquist, an Associate Editor, Brian Henn, Werner Eugster, and an anonymous reviewer) for their thoughtful comments that greatly improved this manuscript. This study was funded by the U.S. Forest Service, the Wyoming Water Development Commission, the USGS, and the NSF (awards EPS-1208909 and EAR-0444053). All data, source code, and statistical results (i.e., posterior distributions) are available at https://doi.org/10.2737/RDS-2018-0032.

References

Advanced Research Computing Center (2012). *Mount Moran: IBM System X cluster*. Laramie, WY: University of Wyoming. Retrieved from http://n2t.net/ark:/85786/m4159

Andreadis, K. M., Storck, P., & Lettenmaier, D. P. (2009). Modeling snow accumulation and ablation processes in forested environments. *Water Resources Research*, *45*, W05429. https://doi.org/10.1029/2008WR007042

Aplet, G. H., Laven, R. D., & Smith, F. W. (1988). Patterns of community dynamics in Colorado Engelmann spruce-subalpine fir forests. *Ecology*, *69*(2), 312–319. https://doi.org/10.2307/1940429

Aubin, I., Beaudet, M., & Messier, C. (2000). Light extinction coefficients specific to the understory vegetation of the southern boreal forest, Quebec. *Canadian Journal of Forest Research*, *30*(1), 168–177. https://doi.org/10.1139/x99-185

Bearup, L. A., Maxwell, R. M., Clow, D. W., & McCray, J. E. (2014). Hydrological effects of forest transpiration loss in bark beetle-impacted watersheds. *Nature Climate Change*, *4*(6), 481–486. https://doi.org/10.1038/nclimate2198

Berryman, E. M., Frank, J. M., Massman, W. J., & Ryan, M. G. (2018). Using a Bayesian framework to account for advection in seven years of snowpack CO_2 fluxes in a mortality-impacted subalpine forest. *Agricultural and Forest Meteorology*, *249*, 420–433. https://doi.org/10.1016/j.agrformet.2017.11.004

Bethlahmy, N. (1974). More streamflow after a bark beetle epidemic. *Journal of Hydrology*, *23*(3–4), 185–189. https://doi.org/10.1016/0022-1694(74)90001-8

Bethlahmy, N. (1975). A Colorado episode: Beetle epidemic, ghost forests, more streatmflow. *Northwest Science*, *49*(2), 95–105.

Bewley, D., Alila, Y., & Varhola, A. (2010). Variability of snow water equivalent and snow energetics across a large catchment subject to mountain pine beetle infestation and rapid salvage logging. *Journal of Hydrology*, *388*(3–4), 464–479. https://doi.org/10.1016/j.jhydrol.2010.05.031

Biederman, J. A., Brooks, P. D., Harpold, A. A., Gochis, D. J., Gutmann, E., Reed, D. E., Pendall, E., et al. (2014). Multiscale observations of snow accumulation and peak snowpack following widespread, insect-induced lodgepole pine mortality. *Ecohydrology*, *7*(1), 150–162. https://doi.org/10.1002/eco.1342

Biederman, J. A., Harpold, A. A., Gochis, D. J., Ewers, B. E., Reed, D. E., Papuga, S. A., & Brooks, P. D. (2014). Increased evaporation following widespread tree mortality limits streamflow response. *Water Resources Research*, *50*, 5395–5409. https://doi.org/10.1002/2013WR014994

Biederman, J. A., Somor, A. J., Harpold, A. A., Gutmann, E. D., Breshears, D. D., Troch, P. A., Gochis, D. J., et al. (2015). Recent tree die-off has little effect on streamflow in contrast to expected increases from historical studies. *Water Resources Research*, *51*, 9775–9789. https://doi.org/10.1002/2015WR017401

Boucher, T. V., & Mead, B. R. (2006). Vegetation change and forest regeneration on the Kenai Peninsula, Alaska following a spruce beetle outbreak, 1987–2000. *Forest Ecology and Management*, *227*(3), 233–246. https://doi.org/10.1016/j.foreco.2006.02.051

Bradford, J. B., Birdsey, R. A., Joyce, L. A., & Ryan, M. G. (2008). Tree age, disturbance history, and carbon stocks and fluxes in subalpine Rocky Mountain forests. *Global Change Biology*, *14*(12), 2882–2897. https://doi.org/10.1111/j.1365-2486.2008.01686.x

Breed, D., Rasmussen, R., Weeks, C., Boe, B., & Deshler, T. (2014). Evaluating winter orographic cloud seeding: Design of the Wyoming Weather Modification Pilot Project (WWMPP). *Journal of Applied Meteorology and Climatology*, *53*(2), 282–299. https://doi.org/10.1175/JAMC-D-13-0128.1

Broxton, P., Harpold, A., Biederman, J., Troch, P., Molotch, N., & Brooks, P. (2015). Quantifying the effects of vegetation structure on snow accumulation and ablation in mixed-conifer forests. *Ecohydrology*, *8*(6), 1073–1094. https://doi.org/10.1002/eco.1565

Brutsaert, W. (1982). *Evaporation into the atmosphere: Theory, history, and applications, D*. Dordrecht, Netherlands: Reidel Publishing Company.

Burba, G. G., McDermitt, D. K., Grelle, A., Anderson, D. J., & Xu, L. K. (2008). Addressing the influence of instrument surface heat exchange on the measurements of CO_2 flux from open-path gas analyzers. *Global Change Biology*, *14*(8), 1854–1876. https://doi.org/10.1111/j.1365-2486.2008.01606.x

Chen, F., Zhang, G., Barlage, M., Zhang, Y., Hicke, J. A., Meddens, A., Zhou, G., et al. (2015). An observational and modeling study of impacts of bark beetle-caused tree mortality on surface energy and hydrological cycles. *Journal of Hydrometeorology*, *16*(2), 744–761. https://doi.org/10.1175/JHM-D-14-0059.1

Cullen, N. J., Mölg, T., Kaser, G., Steffen, K., & Hardy, D. R. (2007). Energy-balance model validation on the top of Kilimanjaro, Tanzania, using eddy covariance data. *Annals of Glaciology*, *46*, 227–233. https://doi.org/10.3189/172756407782871224

van Dijk, A., Kohsiek, W., & de Bruin, H. A. R. (2003). Oxygen sensitivity of krypton and Lyman-α hygrometers. *Journal of Atmospheric and Oceanic Technology*, *20*(1), 143–151. https://doi.org/10.1175/1520-0426(2003)020<0143:OSOKAL>2.0.CO;2

Dormann, C. F., Schymanski, S. J., Cabral, J., Chuine, I., Graham, C., Hartig, F., Kearney, M., et al. (2012). Correlation and process in species distribution models: Bridging a dichotomy. *Journal of Biogeography*, *39*(12), 2119–2131. https://doi.org/10.1111/j.1365-2699.2011.02659.x

Edburg, S. L., Hicke, J. A., Brooks, P. D., Pendall, E. G., Ewers, B. E., Norton, U., Gochis, D., et al. (2012). Cascading impacts of bark beetle-caused tree mortality on coupled biogeophysical and biogeochemical processes. *Frontiers in Ecology and the Environment*, *10*(8), 416–424. https://doi.org/10.1890/110173

Essery, R., Pomeroy, J., Parviainen, J., & Storck, P. (2003). Sublimation of snow from coniferous forests in a climate model. *Journal of Climate*, *16*(11), 1855–1864. https://doi.org/10.1175/1520-0442(2003)016<1855:SOSFCF>2.0.CO;2

Frank, J. M., Massman, W. J., Ewers, B. E., Huckaby, L. S., & Negrón, J. F. (2014). Ecosystem CO_2/H_2O fluxes are explained by hydraulically limited gas exchange during tree mortality from spruce bark beetles. *Journal of Geophysical Research: Biogeosciences*, *119*, 1195–1215. https://doi.org/10.1002/2013JG002597

Frank, J. M., Massman, W. J., Swiatek, E., Zimmerman, H. A., & Ewers, B. E. (2016). All sonic anemometers need to correct for transducer and structural shadowing in their velocity measurements. *Journal of Atmospheric and Oceanic Technology*, *33*(1), 149–167. https://doi.org/10.1175/JTECH-D-15-0171.1

Gelfan, A. N., Pomeroy, J. W., & Kuchment, L. S. (2004). Modeling forest cover influences on snow accumulation, sublimation, and melt. *Journal of Hydrometeorology*, *5*(5), 785–803. https://doi.org/10.1175/1525-7541(2004)005<0785:MFCIOS>2.0.CO;2

Gelman, A., Carlin, J. B., Stern, H. S., Dunson, D. B., Vehtari, A., & Rubin, D. B. (2014). *Bayesian data analysis* (3rd ed., p. 661). Boca Raton, FL: CRC Press.

Good, S. P., Soderberg, K., Wang, L., & Caylor, K. K. (2012). Uncertainties in the assessment of the isotopic composition of surface fluxes: A direct comparison of techniques using laser-based water vapor isotope analyzers. *Journal of Geophysical Research*, *117*, D15301. https://doi.org/10.1029/2011JD017168

Gray, S. T., & Andersen, C. (2009). Assessing the future of Wyoming's water resources.

Harpold, A. A., Biederman, J. A., Condon, K., Merino, M., Korgaonkar, Y., Nan, T., Sloat, L. L., et al. (2014). Changes in snow accumulation and ablation following the Las Conchas Forest Fire, New Mexico, USA. *Ecohydrology*, *7*(2), 440–452. https://doi.org/10.1002/eco.1363

Hartig, F., Calabrese, J. M., Reineking, B., Wiegand, T., & Huth, A. (2011). Statistical inference for stochastic simulation models—Theory and application. *Ecology Letters*, *14*(8), 816–827. https://doi.org/10.1111/j.1461-0248.2011.01640.x

Haverd, V., Cuntz, M., Leuning, R., & Keith, H. (2007). Air and biomass heat storage fluxes in a forest canopy: Calculation within a soil vegetation atmosphere transfer model. *Agricultural and Forest Meteorology*, *147*(3–4), 125–139. https://doi.org/10.1016/j.agrformet.2007.07.006

Hedstrom, N. R., & Pomeroy, J. W. (1998). Measurements and modelling of snow interception in the boreal forest. *Hydrological Processes*, *12*(10–11), 1611–1625. https://doi.org/10.1002/(SICI)1099-1085(199808/09)12:10/11<1611::AID-HYP684>3.0.CO;2-4

Helgason, W., & Pomeroy, J. W. (2011). Characteristics of the near-surface boundary layer within a mountain valley during winter. *Journal of Applied Meteorology and Climatology*, *51*(3), 583–597.

Helgason, W., & Pomeroy, J. W. (2012). Problems closing the energy balance over a homogeneous snow cover during midwinter. *Journal of Hydrometeorology*, *13*(2), 557–572. https://doi.org/10.1175/JHM-D-11-0135.1

Hiemstra, C. A., Liston, G. E., & Reiners, W. A. (2006). Observing, modelling, and validating snow redistribution by wind in a Wyoming upper treeline landscape. *Ecological Modelling*, *197*(1–2), 35–51. https://doi.org/10.1016/j.ecolmodel.2006.03.005

Hobbs, N. T., & Hooten, M. B. (2015). *Bayesian models: A statistical primer for ecologists*. Princeton, NJ: Princeton University Press.

Jacobs, J. J., & Brosz, D. J. (1993). Wyoming's water resources. Cooperative Extension Service and Department of Agricultural Economics, College of Agriculture, University of Wyoming.

Kattelmann, R., & Elder, K. (1991). Hydrologic characteristics and water balance of an alpine basin in the Sierra Nevada. *Water Resources Research*, *27*(7), 1553–1562. https://doi.org/10.1029/90WR02771

Kaufmann, M. R., Edminster, C. B., & Troendle, C. A. (1982). Leaf area determinations for subalpine tree species in the central Rocky Mountains. Rocky Mountain Forest and Range Experiment Station, Fort Collins, Colo. (USDA Forest Service Research Paper RM-238).

Kaufmann, M. R., & Troendle, C. A. (1981). The relationship of leaf area and foliage biomass to sapwood conducting area in four subalpine forest tree species. *Forest Science*, *27*(3), 477–482.

Knowles, J. F., Blanken, P. D., Williams, M. W., & Chowanski, K. M. (2012). Energy and surface moisture seasonally limit evaporation and sublimation from snow-free alpine tundra. *Agricultural and Forest Meteorology*, *157*, 106–115. https://doi.org/10.1016/j.agrformet.2012.01.017

Koeniger, P., Hubbart, J. A., Link, T., & Marshall, J. D. (2008). Isotopic variation of snow cover and streamflow in response to changes in canopy structure in a snow-dominated mountain catchment. *Hydrological Processes: An International Journal*, *22*(4), 557–566. https://doi.org/10.1002/hyp.6967

Kongoli, C., Kustas, W. P., Anderson, M. C., Norman, J. M., Alfieri, J. G., Flerchinger, G. N., & Marks, D. (2014). Evaluation of a two-source snow-vegetation energy balance model for estimating surface energy fluxes in a rangeland ecosystem. *Journal of Hydrometeorology*, *15*(1), 143–158. https://doi.org/10.1175/JHM-D-12-0153.1

Kruschke, J. (2014). *Doing Bayesian data analysis: A tutorial with R, JAGS, and Stan*. Waltham, MA: Academic Press.

Laurila, J., & Lauhanen, R. (2010). Moisture content of Norway spruce stump wood at clear cutting areas and roadside storage sites. *Silva Fennica*, *44*(3), 427–434.

Lee, X., Finnigan, J. J., & Paw U, K. T. (2004). Coordinate system and flux bias error. In X. Lee, W. J. Massman, & B. E. Law (Eds.), *Handbook of Micrometeorology* (pp. 33–66). Dordrecht, Netherlands: Kluwer Academic Publishers.

Leuning, R., van Gorsel, E., Massman, W. J., & Isaac, P. R. (2012). Reflections on the surface energy imbalance problem. *Agricultural and Forest Meteorology*, *156*, 65–74. https://doi.org/10.1016/j.agrformet.2011.12.002

Livneh, B., Deems, J. S., Buma, B., Barsugli, J. J., Schneider, D., Molotch, N. P., Wolter, K., et al. (2015). Catchment response to bark beetle outbreak and dust-on-snow in the Colorado Rocky Mountains. *Journal of Hydrology*, *523*, 196–210. https://doi.org/10.1016/j.jhydrol.2015.01.039

Lu, D., Ye, M., & Hill, M. C. (2012). Analysis of regression confidence intervals and Bayesian credible intervals for uncertainty quantification. *Water Resources Research*, *48*, W09521. https://doi.org/10.1029/2011WR011289

MacClune, K. L., Fountain, A. G., Kargel, J. S., & MacAyeal, D. R. (2003). Glaciers of the McMurdo dry valleys: Terrestrial analog for Martian polar sublimation. *Journal of Geophysical Research*, *108*(E4), 5031. https://doi.org/10.1029/2002JE001878

Mahat, V., & Tarboton, D. G. (2014). Representation of canopy snow interception, unloading and melt in a parsimonious snowmelt model. *Hydrological Processes*, *28*(26), 6320–6336. https://doi.org/10.1002/hyp.10116

Mahat, V., Tarboton, D. G., & Molotch, N. P. (2013). Testing above- and below-canopy representations of turbulent fluxes in an energy balance snowmelt model. *Water Resources Research*, *49*, 1107–1122. https://doi.org/10.1002/wrcr.20073

Mahrt, L., & Vickers, D. (2005). Moisture fluxes over snow with and without protruding vegetation. *Quarterly Journal of the Royal Meteorological Society*, *131*(607), 1251–1270. https://doi.org/10.1256/qj.04.66

Marks, D., Reba, M., Pomeroy, J., Link, T., Winstral, A., Flerchinger, G., & Elder, K. (2008). Comparing simulated and measured sensible and latent heat fluxes over snow under a pine canopy to improve an energy balance snowmelt model. *Journal of Hydrometeorology*, *9*(6), 1506–1522. https://doi.org/10.1175/2008JHM874.1

Massman, W. J. (1992). A surface-energy balance method for partitioning evapotranspiration data into plant and soil components for a surface with partial canopy cover. *Water Resources Research*, *28*(6), 1723–1732. https://doi.org/10.1029/92WR00217

Massman, W. J. (1999). A model study of kB(H)(−1) for vegetated surfaces using “localized near-field” Lagrangian theory. *Journal of Hydrology*, *223*(1–2), 27–43. https://doi.org/10.1016/S0022-1694(99)00104-3

Massman, W. J. (2000). A simple method for estimating frequency response corrections for eddy covariance systems. *Agricultural and Forest Meteorology*, *104*(3), 185–198. https://doi.org/10.1016/S0168-1923(00)00164-7

Massman, W. J. (2004). Toward an ozone standard to protect vegetation based on effective dose: A review of deposition resistances and a possible metric. *Atmospheric Environment*, *38*(15), 2323–2337. https://doi.org/10.1016/j.atmosenv.2003.09.079

McElreath, R. (2016). *Statistical rethinking: A Bayesian course with examples in R and Stan* (1st ed., p. 469). Boca Raton, FL: Chapman and Hall/CRC. https://doi.org/10.1201/9781315372495

Meek, D. W., Prueger, J. H., & Sauer, T. J. (1998). Solutions for three regression problems commonly found in meteorological data analysis. Paper presented at 23rd Conference on Agricultural Forest Meteorology, American Meteorological Society, Albuquerque, NM, November 2-7, 1998.

Millar, D. J., Ewers, B. E., Mackay, D. S., Peckham, S. D., Reed, D. E., & Sekoni, A. (2017). Improving ecosystem-scale modeling of evapotranspiration using ecological mechanisms that account for compensatory responses following disturbance. *Water Resources Research*, *53*, 7853–7868. https://doi.org/10.1002/2017WR020823

Moderow, U., Feigenwinter, C., & Bernhofer, C. (2007). Estimating the components of the sensible heat budget of a tall forest canopy in complex terrain. *Boundary-Layer Meteorology*, *123*(1), 99–120. https://doi.org/10.1007/s10546-006-9136-7

Moeser, D., Mazzotti, G., Helbig, N., & Jonas, T. (2016). Representing spatial variability of forest snow: Implementation of a new interception model. *Water Resources Research*, *52*, 1208–1226. https://doi.org/10.1002/2015WR017961

Molotch, N. P., Blanken, P. D., Williams, M. W., Turnipseed, A. A., Monson, R. K., & Margulis, S. A. (2007). Estimating sublimation of intercepted and sub-canopy snow using eddy covariance systems. *Hydrological Processes*, *21*(12), 1567–1575. https://doi.org/10.1002/hyp.6719

Musselman, K. N., Pomeroy, J. W., & Link, T. E. (2015). Variability in shortwave irradiance caused by forest gaps: Measurements, modelling, and implications for snow energetics. *Agricultural and Forest Meteorology*, *207*, 69–82. https://doi.org/10.1016/j.agrformet.2015.03.014

Musselman, R. C. (1994). The Glacier Lakes Ecosystem Experiments Site. USDA Forest Service, Rocky Mountain Forest and Range Experiment Station, General Technical Report RM–249.

Myneni, R. B., Hoffman, S., Knyazikhin, Y., Privette, J. L., Glassy, J., Tian, Y., Wang, Y., et al. (2002). Global products of vegetation leaf area and fraction absorbed PAR from year one of MODIS data. *Remote Sensing of Environment*, *83*(1–2), 214–231. https://doi.org/10.1016/S0034-4257(02)00074-3

Nakai, Y., Sakamoto, T., Terajima, T., Kitamura, K., & Shirai, T. (1999). Energy balance above a boreal coniferous forest: A difference in turbulent fluxes between snow-covered and snow-free canopies. *Hydrological Processes*, *13*(4), 515–529. https://doi.org/10.1002/(SICI)1099-1085(199903)13:4<515::AID-HYP712>3.0.CO;2-J

Nikolov, N., & Zeller, K. (2006). Efficient retrieval of vegetation leaf area index and canopy clumping factor from satellite data to support pollutant deposition assessments. *Environmental Pollution*, *141*(3), 539–549. https://doi.org/10.1016/j.envpol.2005.08.059

Noone, D., Galewsky, J., Sharp, Z. D., Worden, J., Barnes, J., Baer, D., Bailey, A., et al. (2011). Properties of air mass mixing and humidity in the subtropics from measurements of the D/H isotope ratio of water vapor at the Mauna Loa observatory. *Journal of Geophysical Research*, *116*, D22113. https://doi.org/10.1029/2011JD015773

Noone, D., Risi, C., Bailey, A., Berkelhammer, M., Brown, D. P., Buenning, N., Gregory, S., et al. (2013). Determining water sources in the boundary layer from tall tower profiles of water vapor and surface water isotope ratios after a snowstorm in Colorado. *Atmospheric Chemistry and Physics*, *13*(3), 1607–1623. https://doi.org/10.5194/acp-13-1607-2013

Norton, U., Ewers, B. E., Borkhuu, B., Brown, N. R., & Pendall, E. (2015). Soil nitrogen five years after bark beetle infestation in lodgepole pine forests. *Soil Science Society of America Journal*, *79*(1), 282–293. https://doi.org/10.2136/sssaj2014.05.0223

Penman, H. L. (1948). Natural evaporation from open water, bare soil and grass. *Proceedings of the Royal Society of London. Series A: Mathematical and Physical Sciences*, *193*(1032), 120–145.

Plummer, M. (2003). JAGS: A program for analysis of Bayesian graphical models using Gibbs sampling. Paper presented at Proceedings of the 3rd International Workshop on Distributed Statistical Computing (DSC 2003) March 20–22, Vienna, Austria, Technische Universit at Wien, Vienna, Austria, March 20-22.

Plummer, M. (2011). Generating data from a stochastic model. JAGS: Just Another Gibbs Sampler, Sourceforge. Retrived from https://sourceforge.net/p/mcmc-jags/discussion/610037/thread/71466030/, accessed July 14, 2016.

Plummer, M. (2015a). Cuts in Bayesian graphical models. *Statistics and Computing*, *25*(1), 37–43. https://doi.org/10.1007/s11222-014-9503-z

Plummer, M. (2015b). Rjags: Bayesian graphical models using MCMC. Version 4–4, R Package. Retrieved from http://CRAN.R-project.org/package=rjags

Plummer, M., Best, N., Cowles, K., & Vines, K. (2006). CODA: Convergence Diagnosis and Output Analysis forMCMC. RNews, Vol. 6 (1), R Foundation, Vienna, Austria, 7–11. Retrieved from https://www.r-project.org/doc/Rnews/Rnews_2006-1.pdf

Pomeroy, J. W., & Essery, R. L. H. (1999). Turbulent fluxes during blowing snow: Field tests of model sublimation predictions. *Hydrological Processes*, *13*(18), 2963–2975. https://doi.org/10.1002/(SICI)1099-1085(19991230)13:18<2963::AID-HYP11>3.0.CO;2-9

Pomeroy, J. W., Gray, D. M., Brown, T., Hedstrom, N. R., Quinton, W. L., Granger, R. J., & Carey, S. K. (2007). The cold regions hydrological model: A platform for basing process representation and model structure on physical evidence. *Hydrological Processes*, *21*(19), 2650–2667. https://doi.org/10.1002/hyp.6787

Pomeroy, J. W., Parviainen, J., Hedstrom, N., & Gray, D. M. (1998). Coupled modelling of forest snow interception and sublimation. *Hydrological Processes*, *12*(15), 2317–2337. https://doi.org/10.1002/(SICI)1099-1085(199812)12:15<2317::AID-HYP799>3.0.CO;2-X

Pomeroy, J. W., & Schmidt, R. A. (1993). The use of fractal geometry in modeling intercepted snow accumulation and sublimation. In M. Ferrick & T. Pangburn (Eds.), *Proceedings of the sixty-first annual Western Snow Conference*. Western Snow Conference.

Pugh, E., & Gordon, E. (2013). A conceptual model of water yield effects from beetle-induced tree death in snow-dominated lodgepole pine forests. *Hydrological Processes*, *27*(14), 2048–2060. https://doi.org/10.1002/hyp.9312

Pugh, E., & Small, E. (2012). The impact of pine beetle infestation on snow accumulation and melt in the headwaters of the Colorado River. *Ecohydrology*, *5*(4), 467–477. https://doi.org/10.1002/eco.239

R Core Team (2015). *R: A language and environment for statistical computing*. Vienna, Austria: R Foundation for Statistical Computing. Retrieved from https://www.R-project.org

Raffa, K. F., Aukema, B. H., Bentz, B. J., Carroll, A. L., Hicke, J. A., Turner, M. G., & Romme, W. H. (2008). Cross-scale drivers of natural disturbances prone to anthropogenic amplification: The dynamics of bark beetle eruptions. *Bioscience*, *58*(6), 501–517. https://doi.org/10.1641/B580607

Reba, M. L., Pomeroy, J., Marks, D., & Link, T. E. (2012). Estimating surface sublimation losses from snowpacks in a mountain catchment using eddy covariance and turbulent transfer calculations. *Hydrological Processes*, *26*(24), 3699–3711. https://doi.org/10.1002/hyp.8372

Reed, D. E., Ewers, B. E., & Pendall, E. (2014). Impact of mountain pine beetle induced mortality on forest carbon and water fluxes. *Environmental Research Letters*, *9*(10), 105004. https://doi.org/10.1088/1748-9326/9/10/105004

Ross, J. (1975). Radiative transfer in plant communities. *Vegetation and the Atmosphere*, 13–55.

RStudio Team (2015). *RStudio: Integrated development for R*. Boston, MA: RStudio, Inc. URL http://www.rstudio.com/

Rutter, N., Essery, R., Pomeroy, J., Altimir, N., Andreadis, K., Baker, I., Barr, A., et al. (2009). Evaluation of forest snow processes models (SnowMIP2). *Journal of Geophysical Research*, *114*, D06111. https://doi.org/10.1029/2008JD011063

Santaren, D., Peylin, P., Viovy, N., & Ciais, P. (2007). Optimizing a process-based ecosystem model with eddy-covariance flux measurements: A pine forest in southern France. *Global Biogeochemical Cycles*, *21*, GB2013. https://doi.org/10.1029/2006GB002834

Schlaepfer, D. R., Ewers, B. E., Shuman, B. N., Williams, D. G., Frank, J. M., Massman, W. J., & Lauenroth, W. K. (2014). Terrestrial water fluxes dominated by transpiration: Comment. *Ecosphere*, *5*(5), art61. https://doi.org/10.1890/ES13-00391.1

Schmidt, R. A. (1991). Sublimation of snow intercepted by an artificial conifer. *Agricultural and Forest Meteorology*, *54*(1), 1–27. https://doi.org/10.1016/0168-1923(91)90038-R

Sexstone, G. A., Clow, D. W., Fassnacht, S. R., Liston, G. E., Hiemstra, C. A., Knowles, J. F., & Penn, C. A. (2018). Snow sublimation in mountain environments and its sensitivity to forest disturbance and climate warming. *Water Resources Research*, *54*, 1191–1211. https://doi.org/10.1002/2017WR021172

Shinker, J. J., Shuman, B. N., Minckley, T. A., & Henderson, A. K. (2010). Climatic shifts in the availability of contested waters: A long-term perspective from the headwaters of the North Platte River. *Annals of the Association of American Geographers*, *100*(4), 866–879. https://doi.org/10.1080/00045608.2010.500196

Shuttleworth, W. J., & Wallace, J. S. (1985). Evaporation from sparse crops-an energy combination theory. *Quarterly Journal of the Royal Meteorological Society*, *111*(469), 839–855. https://doi.org/10.1002/qj.49711146910

Speckman, H. N., Frank, J. M., Bradford, J. B., Miles, B. L., Massman, W. J., Parton, W. J., & Ryan, M. G. (2015). Forest ecosystem respiration estimated from eddy covariance and chamber measurements under high turbulence and substantial tree mortality from bark beetles. *Global Change Biology*, *21*(2), 708–721. https://doi.org/10.1111/gcb.12731

Spiegelhalter, D. J., Best, N. G., Carlin, B. P., & van der Linde, A. (2002). Bayesian measures of model complexity and fit. *Journal of the Royal Statistical Society, Series B: Statistical Methodology*, *64*(4), 583–639. https://doi.org/10.1111/1467-9868.00353

Storck, P., Lettenmaier, D. P., & Bolton, S. M. (2002). Measurement of snow interception and canopy effects on snow accumulation and melt in a mountainous maritime climate, Oregon, United States. *Water Resources Research*, *38*(11), 1223. https://doi.org/10.1029/2002WR001281

Stoy, P. C., Mauder, M., Foken, T., Marcolla, B., Boegh, E., Ibrom, A., Arain, M. A., et al. (2013). A data-driven analysis of energy balance closure across FLUXNET research sites: The role of landscape scale heterogeneity. *Agricultural and Forest Meteorology*, *171–172*, 137–152.

Strasser, U., Bernhardt, M., Weber, M., Liston, G., & Mauser, W. (2008). Is snow sublimation important in the alpine water balance? *The Cryosphere*, *2*(1), 53–66. https://doi.org/10.5194/tc-2-53-2008

Sturm, M., Holmgren, J., König, M., & Morris, K. (1997). The thermal conductivity of seasonal snow. *Journal of Glaciology*, *43*(143), 26–41.

Suzuki, K., & Nakai, Y. (2008). Canopy snow influence on water and energy balances in a coniferous forest plantation in northern Japan. *Journal of Hydrology*, *352*(1–2), 126–138.

Svoma, B. M. (2017). Canopy effects on snow sublimation from a Central Arizona Basin. *Journal of Geophysical Research: Atmospheres*, *122*, 20–46. https://doi.org/10.1002/2016JD025184

TenWolde, A., McNatt, J. D., & Krahn, L. (1988). Thermal properties of wood and wood panel products for use in buildings, Rep. Oak Ridge National Lab., TN; Forest Service, Madison, WI. Forest Products Lab.

Thayer, D., Parsekian, A. D., Hyde, K., Speckman, H. N., Beverly, D., Ewers, B. E., Covalt, M., et al. (2018). Geophysical measurements to determine the hydrologic partitioning of snowmelt on a snow-dominated subalpine hillslope. *Water Resources Research*, *54*, 3788–3808. https://doi.org/10.1029/2017WR021324

Troendle, C. A., & King, R. M. (1985). The effect of timber harvest on the Fool Creek watershed, 30 years later. *Water Resources Research*, *21*(12), 1915–1922. https://doi.org/10.1029/WR021i012p01915

Twine, T. E., Kustas, W. P., Norman, J. M., Cook, D. R., Houser, P. R., Meyers, T. P., Prueger, J. H., et al. (2000). Correcting eddy-covariance flux underestimates over a grassland. *Agricultural and Forest Meteorology*, *103*(3), 279–300. https://doi.org/10.1016/S0168-1923(00)00123-4

Veblen, T. T., Hadley, K. S., Reid, M. S., & Rebertus, A. J. (1991). The response of subalpine forests to spruce beetle outbreak in Colorado. *Ecology*, *72*(1), 213–231. https://doi.org/10.2307/1938916

Vickers, D., & Mahrt, L. (1997). Quality control and flux sampling problems for tower and aircraft data. *Journal of Atmospheric and Oceanic Technology*, *14*(3), 512–526. https://doi.org/10.1175/1520-0426(1997)014<0512:QCAFSP>2.0.CO;2

Webb, E. K., Pearman, G. I., & Leuning, R. (1980). Correction of flux measurements for density effects due to heat and water vapour transfer. *Quarterly Journal of the Royal Meteorological Society*, *106*(447), 85–100. https://doi.org/10.1002/qj.49710644707

Welch, C. M., Stoy, P. C., Rains, F. A., Johnson, A. V., & McGlynn, B. L. (2015). The impacts of mountain pine beetle disturbance on the energy balance of snow during the melt period. *Hydrological Processes*, *30*, 588–602. https://doi.org/10.1002/hyp.10638

Williams, D. G., Cable, W., Hultine, K., Hoedjes, J. C. B., Yepez, E. A., Simonneaux, V., Er-Raki, S., et al. (2004). Evapotranspiration components determined by stable isotope, sap flow and eddy covariance techniques. *Agricultural and Forest Meteorology*, *125*(3–4), 241–258. https://doi.org/10.1016/j.agrformet.2004.04.008

Wilson, K., Goldstein, A., Falge, E., Aubinet, M., Baldocchi, D., Berbigier, P., Bernhofer, C., et al. (2002). Energy balance closure at FLUXNET sites. *Agricultural and Forest Meteorology*, *113*(1–4), 223–243. https://doi.org/10.1016/S0168-1923(02)00109-0

Wyoming Water Development Commission (2014). The Wyoming weather modification pilot program—Level II study, draft executive summary, NCAR.

Yamazaki, T. (2001). A one-dimensional land surface model adaptable to intensely cold regions and its applications in eastern Siberia. *Journal of the Meteorological Society of Japan. Series II*, *79*(6), 1107–1118.

Yang, W., Guo, X., Yao, T., Yang, K., Zhao, L., Li, S., & Zhu, M. (2011). Summertime surface energy budget and ablation modeling in the ablation zone of a maritime Tibetan glacier. *Journal of Geophysical Research*, *116*, D14116. https://doi.org/10.1029/2010JD015183

Zhang, Y., Ishikawa, M., Ohata, T., & Oyunbaatar, D. (2008). Sublimation from thin snow cover at the edge of the Eurasian cryosphere in Mongolia. *Hydrological Processes*, *22*(18), 3564–3575. https://doi.org/10.1002/hyp.6960

Zhang, Y., Suzuki, K., Kadota, T., & Ohata, T. (2004). Sublimation from snow surface in southern mountain taiga of eastern Siberia. *Journal of Geophysical Research*, *109*, D21103. https://doi.org/10.1029/2003JD003779